

# Proof-of-Authorship for Diffusion-based AI Generated Content

De Zhang Lee  
*National University of Singapore*

Han Fang  
*National University of Singapore*

Ee-Chien Chang  
*National University of Singapore*

## Abstract

Recent advancements in AI-generated content (AIGC) have introduced new challenges in intellectual property protection and the authentication of generated objects. We focus on scenarios in which an author seeks to assert authorship of an object generated using latent diffusion models (LDMs), in the presence of adversaries who attempt to falsely claim authorship of objects they did not create. While proof-of-ownership has been studied in the context of multimedia content through techniques such as time-stamping and watermarking, these approaches face notable limitations. In contrast to traditional content creation sources (e.g., cameras), the LDM generation process offers greater control to the author. Specifically, the random seed used during generation can be deliberately chosen. By binding the seed to the author’s identity using cryptographic pseudorandom functions, the author can assert to be the creator of the object. We refer to this stronger guarantee as proof-of-authorship, since only the creator of the object can legitimately claim the object. This contrasts with proof-of-ownership via time-stamping or watermarking, where any entity could potentially claim ownership of an object by being the first to timestamp or embed the watermark. We propose a proof-of-authorship framework involving a probabilistic adjudicator who quantifies the probability that a claim is false. Furthermore, unlike prior approaches, the proposed framework does not involve any secret. We explore various attack scenarios and analyze design choices using Stable Diffusion 2.1 (SD2.1) as representative case studies.

## 1 Introduction

Latent diffusion models (LDMs) such as Stable Diffusion, DALL-E, and Midjourney, have gained prominence for their ability to generate remarkably high-quality images from textual descriptions. Generating such images require significant prompt engineering and tuning effort on the part of the author, and it is in the author’s interest to protect their generated content against misattribution. Although there are debates on

whether AI generated object should be eligible for copyright protection [5], it is generally a consensus that authorship of AI generated content should belong to the user who created it [4, 49].

There are several well-known proof-of-ownership approaches that enable an author to claim ownership of digital objects. One widely used approach is time-stamping, where an owner claims ownership of an object by publicly time-stamping the object with a digital signature. However, this method alone is insufficient, as it is possible for anyone to timestamp any object without being its author, but by being the first to claim authorship publicly.

Another approach is digital watermarking, in which the author embeds a secret watermark into the objects, and the author can later prove ownership by demonstrating knowledge of this secret. There are two groups of techniques in embedding the watermarks. One could employ pixel-based methods that embed the watermark in the pixel domain. Nonetheless, straightforward adoptions are vulnerable to ambiguity attacks, where an adversary inverts and forges another secret watermark that happens to be in the object, resulting in an ambiguous situation where both the owner and the adversary can plausibly claim authorship [7]. While such attacks can be mitigated by applying a cryptographic hash to the secret before embedding [29], watermarking still faces inherent vulnerability to removal attacks. The secret watermark can also be embedded through inversion (or latent)-based watermarking [14, 50, 53] whereby objects are generated with randomness derived from some secret. For example, the starting point is sampled from a distribution parameterized by a secret key, as in Gaussian Shading [53] or Pseudorandom Error Correcting Code (PRC) watermark [14]. Similar to pixel-based watermarking, without additional protection, an adversary might be able to carry out ambiguity attack. Furthermore, both pixel and latent-based watermarks relies on an author’s secret to prove ownership. Although zero-knowledge proofs can be incorporated to protect such secrets, [12], verification is computationally expensive, especially for the high-dimensional objects.

In this paper, we show that a simple lightweight mechanism that does not rely on any secret is sufficient for proof-of-ownership. In fact, the mechanism achieves beyond proof-of-ownership in the sense that only objects generated by LDM by the author can be claimed, in contrast to proof-of-ownership whereby existing known objects could be claimed. Hence, we refer to this as a proof-of-authorship (POA) framework. Under this framework, the random starting point of the LDM is cryptographically bound to the author’s identity and some generation meta-data. Specifically, the seed used to sample the random starting point is obtained by feeding authorship information, such as the author’s identity, prompt, and model version, into a cryptographically secure pseudorandom function (PRF). To claim authorship of an object  $I$ , the author demonstrates that  $I$  is similar to an object generated using a starting point bound to the author, and with high statistical confidence, the probability  $\alpha$  of a randomly generated object which happens to resemble  $I$  is extremely small. Furthermore, via cryptographic binding, no probabilistic polynomial-time adversary can outperform random guessing when forging such authorship information.

While the framework is conceptually simple, it involves several subtle challenges. First, although LDM generation is complex, it does not constitute a cryptographic one-way function, raising the possibility that certain inversion attacks may be feasible. Second, because the claim relies on statistical hypotheses over rare events, it is unclear whether the associated statistical tests can be conducted with high confidence when only small sample sizes are available.

We propose that, in addition to the well-accepted hardness assumptions on PRFs (Assumption A1 in Section 3.2), one should impose an additional assumption on the statistical properties of LDM (Assumption A2 in Section 3.2). Specifically, we assume that the similarity measure of truly randomly generated objects follows a sub-exponential distribution. This is arguably a weak assumption and holds in practice because by design, LDMs generated objects that follow a multivariate Gaussian distribution. Since similarity measure follow the form of cosine similarity, this further leads to a sub-exponential distribution.

The first assumption (A1) reduces any adversary’s strategy to random guessing, even if the adversary can invert LDM. The second assumption (A2) is imposed for efficiency, as it enables statistical testing on rare events with a small sample size. In cases where Assumption A2 does not hold (for instance, if the LDM contains backdoors) we can show that the adversary still cannot succeed provided that the verifier has computational resources comparable to those of the adversary.

We introduce a Probabilistic Adjudicator (PA) to conduct statistical tests and a Judge to determine whether the parameters are reasonable. However, this division of responsibilities may vary across application scenarios.

*Contributions.* Our contributions are as follows:



(a) Original (b) JPEG (quality 1)

Figure 1: The similarity score between the original and distorted image is  $T = 8.6$ . For any forger who is unable to break the pseudorandom function, the probability of generating an image whose similarity score with the contested image meets or exceeds  $T$  in a single attempt is at most  $2^{-50}$ . This implies that the identity cryptographically bound to original image is likely not forged, and therefore corresponds to the legitimate author.

1. We propose a lightweight proof-of-authorship framework for LDM generated content that does not require the authors to keep secrets, and provide more assurance than proof-of-ownership. We propose imposing an assumption on the LDM (Assumption A2) for efficient statistical testing.
2. We show that:
  - (a) No probabilistic polynomial-time adversary can outperform random guessing when attempting to forge a claim.
  - (b) Under Assumption A2, only a small number of samples (compared to naive sampling) is needed to statistically determine whether a claim is valid.
  - (c) The proposed authorship verification test is statistically optimal.
3. We evaluate our approach on Stable Diffusion 2.1 and show that reasonable security parameters are attainable. For typically generated objects and a target random forger’s attack success probability of  $2^{-50}$ , our method attains accuracy of 100% when determining whether an object corresponds to a given author. Moreover, even under distortions (see Figure 1 for an example), the probability that a forger successfully forges a claim remains below  $2^{-50}$ .

## 2 Background and Notations

### 2.1 Latent-Diffusion model

A LDM takes in meta-parameter  $m$  (e.g., type of scheduler, number of timesteps, etc.), an embedding  $e$  generated from

a prompt  $p$  (for e.g., in SD 2.1,  $e$  a real vector of dimension  $n_p \times 77 \times 1,024$  where  $n_p$  is a integer dependent on  $p$ ), and a starting point  $s$  in the latent space (e.g., in SD 2.1, this is a vector in  $\mathbb{R}^{4 \times 64 \times 64}$ ), and outputs the generated image  $L_m(e, s)$ .

The authors are typically oblivious to the numeric values in the embedding  $e$ . Instead, an author would provide a text prompt which is then converted to an embedding  $e$  through a text encoder. For e.g., the CLIP Tokenizer converts a text to the real vector of the embedding  $e$  of dimensions  $n_p \times 77 \times 1,024$ , where  $n_p$  is the number of tokens in the prompt.

The starting latent point is randomly generated following a distribution  $\mathcal{D}_0$  suitable for the diffusion process, for e.g., a multivariate Gaussian distribution. This starting point can be generated using some pseudorandom number sampling  $G : \{0, 1\}^{n_{seed}} \rightarrow \mathcal{L}$  that maps a binary sequence of length  $n_{seed}$  to a point in the latent-space  $\mathcal{L}$ , such that the output distribution  $\mathcal{D}_0$  approximates the desired multivariate Gaussian distribution when the seeds are uniformly chosen. Small amounts of noise is iteratively removed over several timesteps, conditional on the prompt and LDM parameters, resulting in a latent-space representation of the image. Finally, this latent-space representation is upscaled into an actual image (typically of a higher dimension) using a variational autoencoder (VAE).

To create an image, an author could experiment with different prompts, seeds and meta parameters to derive a desired generated object  $L_m(e, s)$ , where  $e$  is the embedding derived from the prompt,  $s$  is the starting latent point generated from the seed, and  $m$  is the meta parameter. To summarize, from the author’s perspective, with  $m$ ,  $p$  and a *seed*, the generated image is  $L_m(e, s)$ , where  $e = \text{CLIP}(p)$  and  $s = G(\text{seed})$ .

The effect by  $e$  is significant as it corresponds to the semantics of the generated content, whereas  $m$  corresponds to the visual quality, and different starting points  $s$  lead to different generated content with similar semantics. As a function, the LDM is assumed to admit some “smoothness” properties, in the sense that a slight perturbation of  $e$ ,  $s$  and  $m$  will lead to small perturbations of the image in the pixel domain (under the  $\ell_2$ -metric) [15, 30, 52].

### 2.1.1 VAE Autoencoder

In a typical LDM pipeline, the denoised latent is upscaled into an image of higher dimensions using a pretrained VAE. This is for computational efficiency. The VAE encoder maps an image  $x$  into a latent  $z$ , which admits the conditional distribution  $q_\phi(z | x) = \mathcal{N}(z | \mu_x, \sigma_x^2 I)$ , where both  $\mu_x$  and  $\sigma_x$  are vectors dependent on  $x$ . Sampling from this distribution yields latent-space representations of images, which decode back into images perceptually similar to the original image  $x$ . Furthermore, VAEs are designed such that the unconditional prior distribution of the latent space  $z$  follows a  $\mathcal{N}(0, I)$  distribution.

## 2.2 Image Similarity Function

Measuring similarity between images in the pixel domain is challenging. Possible similarity functions include the  $\ell_2$  metric or some metric derived from human visual system (see [8] for a survey). However, such metrics are sensitive to certain transformations (e.g. mild geometric transformations or small amounts of noise) which maintain perceptual similarity but induces large distances when these metrics are employed, and may be susceptible to higher false-positive rates.

To capture similarity under reasonable transformations which maintain perceptual similarity, we measure distances in the latent space rather than directly in pixel space. The latent representation provides a lower-dimensional embedding of the image and, and inherent robustness to small perturbations and noise due to the VAE training process [22]. This has been validated empirically in practice, see for example [27, 47].

## 2.3 Pseudorandom function family (PRF)

A pseudorandom function family (PRF) is a class of functions whose outputs cannot be distinguished from a random oracle in polynomial time. A random oracle, on query that it has not seen before, randomly outputs a value sampled from a desired distribution; otherwise (on a previously seen query), outputs the same value for the previously seen query. Many practical constructions, for example, HMAC with SHA, are assumed to be PRF.

In the context of LDMs, one could employ PRF to generate the seeds that are fed into the  $\mathcal{D}_0$  sampler  $G$  to obtain the starting points. By properties of PRF, the composite of the chosen PRF and  $G$  emulates the random oracle that follows  $\mathcal{D}_0$ . Let us denote the class of functions,  $f_i : \{0, 1\}^{n_k} \rightarrow \{0, 1\}^{n_{seed}}$  to be the PRF, where  $i \in I$  for a set of identities  $I$ ,  $n_k$  is the bit length of the input and  $n_{seed}$  is the bit length of the seed. Using the above notations and on assumption that  $\{f_i\}_{i \in I}$  is a PRF, the composite  $(G \circ f_i)$  emulates a random oracle whose output follows  $\mathcal{D}_0$ .

## 2.4 Statistical Testing

We briefly review the statistical testing framework, used to determine if a given author (associated with a unique identifier  $i$ ) and associated set of generation parameters  $\kappa$  corresponds to a contested object  $I$ .

Let  $T$  be the similarity score between  $\mathcal{L}$ , and the object generated corresponding to  $i$  and  $\kappa$ . The PA computes the probability  $q$  that a forger, given  $m$ ,  $e$  and a randomly sampled starting point from  $\mathcal{D}_0$ , generates an object whose similarity score (with respect to  $I$ ) is at least  $T$ . For convenience, let us refer to such a forger as a random forger, and  $q$  as the random forger’s success rate.

**Estimation of  $q$**  In practice, to determine if a random forger is able to achieve a similarity score of  $T$  with a probability of at most  $q$ , a naive empirical approach requires at least  $\frac{1}{q}$  samples, which is expensive for small  $q$ . Instead, we assume that the distribution of the similarity score follows some known distribution, which reduces the problem to that of estimating the distribution parameters and can be achieved with significantly fewer samples. Nonetheless, this introduces estimation errors, which may lead to an under-estimation of  $q$ . In Appendix A, we show that to approximate  $q$  with error of at most  $\alpha$  and statistical confidence of  $1 - \delta$  using our approach, it suffices to use  $n = \Omega(\ln^2 \frac{1}{\alpha} \ln \frac{1}{\delta})$  samples. Henceforth, we denote  $C_\delta = (\hat{q} - \alpha, \hat{q} + \alpha)$  as the  $(1 - \delta)$  confidence interval of  $q$  with width  $2\alpha$ , computed using  $n$  independent samples and  $\hat{q}$  is the point estimate of  $q$ .

## 2.5 Summary of notations

Table 1 presents a summary of notations used, including those introduced later.

Symbol	Description
$m$	Meta-parameters for LDM.
$e$	Embedding.
$s$	Starting point of LDM.
$L_m(e, s)$	LDM generated object.
$G(\cdot)$	Deterministic sampler giving samples of $\mathcal{D}_0$ .
$\mathcal{D}_0$	Starting point distribution.
$f_i(\cdot)$	Pseudorandom function for identity $i$ .
$\text{Sim}(\cdot, \cdot)$	Similarity function.
$T$	Observed similarity score.
$q$	Probability that a random forger attains similarity score at least $T$ .
$\hat{q}$	Point estimate of $q$ .
$C_\delta$	$(1 - \delta)$ confidence interval of $q$ with width $2\alpha$
$\alpha$	Upper bound of estimation error of $q$ with probability of at least $(1 - \delta)$

Table 1: Summary of notations used.

## 3 Proof-of-Authorship Framework

This framework involves several entities: *Author*, *Probabilistic adjudicator*, *Judge* and *forger*; three phrases: *setup*, *generation* and *contention*; and several algorithms: the LDM  $L_m(\cdot, \cdot)$ , similarity function  $\text{Sim}(\cdot, \cdot)$ , the class of cryptographically secure pseudorandom function  $f_i$ 's and pseudorandom number sampling  $G(\cdot)$  as discussed in Section 2, and the statistical test to be carried out by the PA.

## 3.1 Phases

### 3.1.1 Registration

During this phase, each author chooses and publishes a unique identifier  $i \in I$  that serves as the index  $i$  of  $f_i(\cdot)$ . The purpose of registration is to avoid the ambiguous situation where multiple authors have the same identifier.

### 3.1.2 Generation

An author can experiment with various prompts (which determines the embedding), meta-parameters and starting points. In this framework, the starting points are deterministically obtained from the composition  $(G \circ f_i)(\langle m, e, r \rangle)$ , where  $f_i$  is a pseudorandom function (e.g. HMAC-SHA3),  $i$  is the author's identity,  $m$  is the meta-parameter,  $e$  the embedding, and  $r$  a randomly sampled binary sequence. Hence, if  $m$  and  $e$  are fixed, the author  $i$  can randomly sample the starting points by feeding in a random sequence  $r$  to generate multiple objects. An illustration of this generation process is given in Figure 2.

The parameters  $m, e, r$  of an object  $J$  would be archived for further lookup. As it is not necessary to keep  $m, e, r$  as secret, if the author chooses to, they can be pushed to public domains or distributed ledgers. Henceforth, we will use  $\kappa = \langle m, e, r \rangle$  to denote the generation parameters of an object.

### 3.1.3 Contention

This situation arises when an author  $i$  wants to claim authorship of an object  $I$ . For instance, the object  $I$  is an image that appears in the public domain and the author wants to convince others that  $I$  is a slightly distorted and transformed copy of an original image  $J$ . In particular, the author knows  $m, e$  and  $r$  such that  $J = L_m(e, (G \circ f_i)(\langle m, e, r \rangle))$ . Let us call  $J$  the *original* object and call  $I$  the *contested* object. To support the claims, the following is carried out:

1. The author passes the following to the probabilistic adjudicator: contested object  $I$ , the author's identity  $i$ , the generation parameters  $\kappa = \langle m, e, r \rangle$ , a desired error bound  $\alpha$ , statistical confidence  $(1 - \delta)$ , and a transformation  $t$  which aligns the contested and original objects. The PA carries out the statistical test outputs  $\hat{q}$ . The parameter  $\alpha$  and  $q$  represent the range  $C_\delta = (\hat{q} - \alpha, \hat{q} + \alpha)$ , which is the  $(1 - \delta)$  confidence interval of  $q$ . An illustration of the contention phase is given in Figure 3.
2. The PA passes all the information above to the judge, including its inputs,  $\hat{q}$  and  $C_\delta$

**Judge** Using the information provided, the judge outputs an assertion. For instance, if the upper quantile of  $C_\delta$  is small (e.g.  $2^{-50}$ ), it is unlikely that a forger can find such a similar object. The judge may also use other information, e.g. validity of the transformation or other contextual factors.

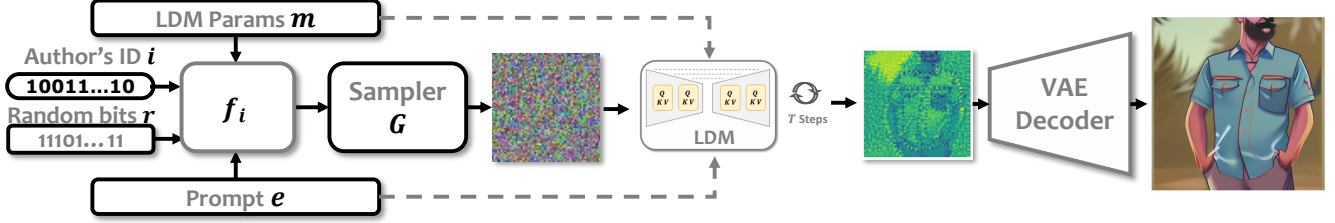


Figure 2: An illustration of the generation phase for the POA  $\langle m, e, r \rangle$ . A pseudorandom function  $f_i$  (e.g. HMAC-SHA3) deterministically maps the POA to a seed that initializes the starting point. The random free bits  $r$  enable sampling from different locations, preserving diversity in the generated outputs.

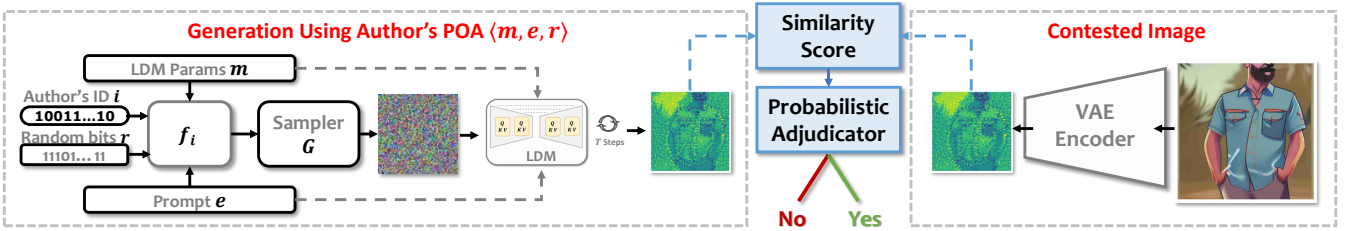


Figure 3: An illustration of the contention phase in our POA framework. The left depicts the VAE latent generated from the POA  $\langle m, e, r \rangle$ , compared against the VAE latent of the contested image (right). A similarity score is computed from the two latents (Section 4.1) and evaluated by the probabilistic adjudicator to determine whether the POA corresponds to the contested image.

Section 3.4 describes the PA and judge in greater detail.

### 3.1.4 Forger

A forger intends to falsely claim authorship of a point of contention  $I$ . The object  $I$  could be generated from LDM or objects from other non-AIGC source (e.g. digital image taken using a camera). In cases where the object is LDM generated, let us assume that the forger knows all the parameters, i.e., the original author's identity  $i$  and corresponding generation parameters  $\kappa = \langle m, e, r \rangle$  that generates  $I$ .

Given  $I$ , the forger wants to find a  $\langle \tilde{m}, \tilde{e}, \tilde{r} \rangle$  s.t. the PA outputs a small  $\hat{q}$ . Since the forger knows  $m$  and  $e$ , the forger could try multiple starting points with  $m$  and  $e$  to find an object similar to  $I$ . Alternatively, the forger could try with different meta-information and embedding.

## 3.2 Security Assumptions

The PA relies on two assumptions, an assumption on the existence of PRF, and statistical properties of the LDM.

- (A1) *Hardness of  $f_i$ 's.* We assume that  $\{f_i\}_{i \in I}$  is a pseudorandom function as discussed in Section 2.3. In our implementation, this is realized by a HMAC with SHA3-256.
- (A2) *Diffusion property on LDM.* We assume that, given any  $i_0, m, e$ , the distribution  $Sim(i_0, L_m(e, S))$  where  $S$  is

sampled from a multivariate Gaussian  $\mathcal{N}(0, I)$ , follows a sub-exponential probability distribution function.

The above assumptions are crucial. By the assumption on computation hardness of PRF (Assumption A1), a forger cannot perform better than the random forger who randomly searches for an alternative set of POA which corresponds to the image in question (Section 3.5).

Leveraging Assumption A2, we can bound the tail probability of  $Sim(i_0, L_m(e, S))$  by estimating the parameters of the underlying sub-exponential distribution. Without this assumption, bounding this tail probability at the  $(1 - q)$ -th quantile with high statistical confidence would require at least  $\frac{1}{q}$  samples, which is prohibitively expensive for small  $q$ , e.g.,  $q = 2^{-30}$ . In contrast, under Assumption A2, this tail probability can be estimated using a small number of samples  $S_1, \dots, S_n \sim \mathcal{D}_0$  by evaluating the similarity scores  $Sim(i_0, L_m(e, S_1)), \dots, Sim(i_0, L_m(e, S_n))$ . We discuss this further in Appendix A.

Regarding Assumption A1, there exists classes of functions that are widely accepted to be PRF and satisfy this assumption.

Regarding Assumption A2, suppose the VAE produces a latent representation consisting of  $d$  independent and identically distributed random variables where  $d$  is large (e.g.  $d = 4 \times 64 \times 64$  in SD2.1). Then, by Lemma 2, Assumption A2 is satisfied.

Empirically, however, latent variables learned by standard VAEs typically exhibit mild statistical dependence, resulting

in small correlations across latent dimensions [6, 21]. By assuming such weak dependence, sums of  $d$  weakly dependent random variables admit a central-limit-type Gaussian approximation under weak dependence (see Theorem 8.2.8 of [9]). Moreover, since each latent component is sub-exponential, their sum remains sub-exponential, and therefore, still satisfies Assumption A2.

### 3.3 Choice of $G \circ f_i$

We choose HMAC SHA3-256 as our choice of PRF, which is widely assumed to meet the PRF requirement. For the sampler  $G$ , we adopt a pseudorandom number generator in the PyTorch library, that on an input seed, outputs pseudorandom samples following the  $\mathcal{N}(0, I)$  distribution. Our security analysis requires the property that, if  $s$  is computationally indistinguishable from a truly random  $s'$ , then  $G(s)$  is computationally indistinguishable from  $G(s')$ . Since this property holds for any deterministic  $G(\cdot)$ , we do not need to impose  $G$  to be a cryptographically secure pseudorandom number generator.

### 3.4 Probabilistic Adjudicator Algorithm

As mentioned in Section 3.1.3, the input to PA are: Contested object  $I$ , transformation  $t$ , generation parameters  $\kappa = \langle m, e, r \rangle$ , author’s ID  $i$ , upper bound of estimation error  $\alpha \in (0, 1)$ , and statistical confidence  $(1 - \delta) \in (0, 1)$ . The PA performs the following steps.

#### Step 0: Determining The Number of Samples Needed

First, the PA generates the original  $J = L_m(e, G(f_i(\kappa)))$ . Recall that  $W$  is the distribution of  $L_m(e, s)$  where  $s \sim \mathcal{D}_0$ . To estimate  $W$ , the PA computes  $n = \ln^2 \frac{1}{\alpha} \ln \frac{1}{\delta}$ , which is the number of Monte-carlo samples needed so that the estimation error of  $\hat{q}$  is at most  $\alpha$  with confidence of at least  $(1 - \delta)$ . Section 3.4.1 gives details on the derivation of  $n$ .

**Step 1: Estimating the Similarity Score Distribution** The PA independently samples  $s_1, \dots, s_n \sim \mathcal{D}_0$ , and generates  $J_1, \dots, J_n$ , where  $J_j = L_m(e, s_j)$ . Subsequently, the PA approximates the empirical distribution  $\hat{W}$  of the Monte-Carlo samples  $\{Sim(J, t(J_j)) : j = 1, \dots, n\}$ , by computing the maximum likelihood estimate of the underlying distribution parameters over these samples. We use the implementation provided by Python’s scipy package to perform this estimate.

**Remark** To ensure reproducibility and prevent the PA from biasing the outcome by selecting randomness favorable to a forger, the PA derives its randomness (i.e. the pseudorandom seed) from a secure deterministic one-way hash (e.g. SHA-256) of its inputs.

**Step 2: Computing  $C_\delta$**  The PA estimates  $\hat{q} = \mathbb{P}[\hat{W} \geq Sim(J, t(I))]$ . With probability of at least  $1 - \delta$ , the error of  $\hat{q}$  is at most  $\alpha$ . Accordingly,  $C_\delta = (\hat{q} - \alpha, \hat{q} + \alpha)$  is a conservative  $(1 - \delta)$  confidence interval of  $q$ .

**Step 3: Output** The PA passes all information above to the judge, including its inputs,  $\hat{q}$  and  $C_\delta$ .

**Judge’s Assertion** The judge uses the information provided by the PA to evaluate the assertion whether the contested object  $I$  originates from the original  $J$ , generated using parameters which are bound to the author. Let  $q'$  be the upper bound of  $C_\delta$ . In our evaluations in Section 5, we simulate a judge by accepting the assertion if  $q'$  is very small (e.g.  $2^{-50}$ ), making it exceedingly unlikely that a random forger could succeed.

**Permissible Transformations** A forger may attempt to evade detection by applying mild, perceptually preserving transformations (e.g., affine transformations like rotation and translation) to the contested object. Accordingly, the the author specifies the transformation  $t$ , which may include the identity transformation. The judge may reject the assertion if the transformation is deemed unreasonable (e.g., if it corresponds to only a small subimage of the original).

**Correctness and Optimality of PA** The PA described computes the test statistic for the hypothesis test formalized in Theorem 2. Since this test is uniformly most powerful, the PA’s assertion is statistically optimal for distinguishing objects corresponding to a given author and generation parameters  $\kappa$ , achieving the theoretically minimal false-negative rate.

#### 3.4.1 Derivation of $n$ and $C_\delta$

Leveraging on Assumption A2, we prove in Theorem 3 in Appendix A that to bound our estimation error of  $q$  by  $\alpha$ , it suffices to use  $n = \Omega(\ln^2 \frac{1}{\alpha} \ln \frac{1}{\delta})$  samples. This result is stated below:

**Theorem 3.** *Under Assumption A2, and standard MLE regularity assumptions, let  $\alpha \in (0, 1)$  and  $\delta \in (0, 1)$  and consider a fixed threshold  $T$ . Let  $\hat{q} = \Pr[\hat{W} \geq T]$ , where  $\hat{W}$  is estimated over  $n$  independently and identically distributed samples drawn from a distribution  $W$ . If  $n \in \Omega(\ln^2 \frac{1}{\alpha} \ln \frac{1}{\delta})$ , then  $\hat{q}$  estimates the true probability  $q = \mathbb{P}[W \geq T]$  within an additive error of  $\alpha$ , with probability at least  $1 - \delta$ .*

Table 2 reports the number of samples required when Assumption A2 is employed, versus naive sampling.

### 3.5 Security Analysis

To recap, suppose an image is generated by an author with identity  $i$  and generation parameters  $\langle m, e, r \rangle$ . The forger’s

$\alpha$	(I) Naive Sampling	(II) Assumption A2 ( $n = \ln^2(1/\alpha) \ln(1/\delta)$ )	Ratio of I:II
$2^{-10}$	$\geq 2^{10}$	$\approx 2^8$	$2^2$
$2^{-30}$	$\geq 2^{30}$	$\approx 2^{12}$	$2^{18}$
$2^{-50}$	$\geq 2^{50}$	$\approx 2^{13}$	$2^{37}$

Table 2: Comparison of sample complexity for determining whether  $q \leq \alpha$  with confidence  $1 - \delta$ , where  $\delta = 0.001$ . Leveraging Assumption A2 reduces the required number of samples from exponential in  $1/\alpha$  to polylogarithmic.

goal is to (1) generate a similar image that can be attributed to the forger’s own identity and generation parameters, or (2) transform the image into a modified version which is similar to the original but cannot be claimed by the author.

In our security analysis, we show that no polynomial-time forger can achieve more than a negligible advantage for the first goal over an adversary limited to random guessing (i.e., a random forger). The second goal corresponds to a *removal attack*, which is addressed in our subsequent analysis of the similarity function.

### 3.5.1 Threat Model

Given a publicly released set of generation parameters  $\kappa = \langle m, e, r \rangle$  associated with an author  $i$  used to generate an object  $I$ , we consider the following classes of adversaries:

1. *Random Forger* (Section 3.5.2): A random forger, conditional on the same  $m, e$  and the forger’s own identity, attempts to find an  $r'$  such that the forged object is similar to the original.
2. *Malicious Forger* (Section 3.5.3): Unlike the random forger, the malicious forger employs a probabilistic polynomial time algorithm to derive generation parameters  $\tilde{\kappa}$  such that, conditional on  $\tilde{\kappa}$  and the forger’s identity, the forged object is similar to the original.
3. *Malicious Model Provider* (Section 3.5.5): The malicious model provider attempts to violate Assumption A2, with the goal of introducing ambiguity in the verification process. For example, the model is constructed a non-negligible proportion of starting points sampled from  $\mathcal{D}_0$  map to similar generated objects, which results in several entities plausibly claiming authorship.
4. *Colluding PA* (Section 3.4): A malicious PA may deliberately manipulate its pseudo-randomness to favor the adversary.

Additionally, in Section 4.2, we consider a removal attack, in which an adversary seeks to evade detection by manipulating the similarity function, so that the contested and original objects remain close under a given distance metric, but their similarity score is reduced.

### 3.5.2 Random Forger

Let us write

$$\tilde{S}_j^{m,e,I}(r) \stackrel{\text{def}}{=} \text{Sim}(L_m(e, (G \circ f_j)(\langle m, e, r \rangle)), I), \quad (1)$$

which denotes the output of the similarity function over an image  $I$  and  $L_m(e, (G \circ f_j)(\langle m, e, r \rangle))$ .  $S_j^{m,e,I}(\cdot)$  follows some distribution when  $r$  is randomly chosen. Definition 1 formally defines the forger’s advantage:

**Definition 1.** Given generation parameters  $\kappa = \langle m, e, r \rangle$  and generated object  $I = L_m(e, f_i(\kappa))$ , let  $S_j^{m,e,I}(r)$  be as defined in (1). Given a forger  $\phi(I, \kappa)$ , which takes as input  $I$  and  $\kappa$ , let  $\tilde{\kappa} = \langle \tilde{m}, \tilde{e}, \tilde{r} \rangle \leftarrow \phi(I, \kappa)$  denote the forged generation parameters. The advantage of  $\phi$  w.r.t.  $I, \kappa$ , is written as:

$$\text{Adv}_\phi(I, \kappa) = \mathbb{P}_{r' \leftarrow \text{Unif}(\cdot)}[S_j^{\tilde{m}, \tilde{e}, I}(\tilde{r}) - S_i^{m,e,I}(r') > 0] - \frac{1}{2},$$

where the probability is over a uniformly sampled  $r'$ ,  $\tilde{r}$  is provided by the forger  $\phi$ , and  $j$  corresponds to the forger’s identity,

$\text{Adv}_\phi(I, \kappa)$  quantifies the extent that the forger  $\phi$  outperforms a random forger. We show in Section 3.5.4 that no forger can outperform a random forger by a non-negligible advantage.

### 3.5.3 Forger’s Attack Goal

Recall that, given an image  $I$  (generated by author  $i$  and generation parameters  $\langle m, e, r \rangle$ ), a forger with identity  $j$  aims to produce a generation parameters  $\langle \tilde{m}, \tilde{e}, \tilde{r} \rangle$ , such that the resulting generated image  $J = L_{\tilde{m}}(\tilde{e}, (G \circ f_j)(\langle \tilde{m}, \tilde{e}, \tilde{r} \rangle))$  is similar to  $I$  but corresponds to the forger’s identity and generation parameters. If this occurs, an *ambiguous scenario* arises: both the original author and the forger possess valid (identity, generation parameters) pairs, namely  $(i, \langle m, e, r \rangle)$  and  $(j, \langle \tilde{m}, \tilde{e}, \tilde{r} \rangle)$ , respectively, which correspond to similar objects  $I$  and  $J$ . Let us call this forger a malicious forger.

Empirically, if an adaptive forger uses a different embedding  $\tilde{e}$  and meta-parameter  $\tilde{m}$  compared to the original  $e$  and  $m$ , the forged object  $J$ , while possibly semantically similar, will be significantly different compared  $I$  (see [43] for the empirical results). Since the forger already knows the original  $m$  and  $e$ , it would be more efficient for the forger to use them during the search. That is, the forger explores  $J = L_m(e, (G \circ f_j)(\langle m, e, \tilde{r} \rangle))$ , i.e. objects corresponding to  $I$ ’s original embedding  $e$  and meta-parameters  $m$ , while varying the randomly sampled initialization point controlled by  $\tilde{r}$ .

### 3.5.4 Impossibility of a Polynomial-time Forger

Under the PRF Assumption A1, no probabilistic polynomial-time (PPT) forger can achieve a non-negligible advantage over

a random forger (with respect to the security parameter of the PRF family). This result is formally stated in Theorem 1. The full proof is deferred to Appendix B, and we present a sketch here.

**Theorem 1.** *Under the PRF assumption, for all PPT forger  $\phi$ ,  $I$ ,  $\text{Adv}_\phi(I, \kappa) \leq \text{negl}(\lambda)$ , where  $\lambda$  is the security parameter of the PRF family.*

**Proof Sketch.** By the PRF assumption, for any PPT adversary that has not queried  $f_i(\kappa)$ ,  $f_i(\kappa)$  is computationally indistinguishable from a truly-random sequence. This holds even if the adversary is allowed a polynomial number of queries to  $f_i$  (excluding the input  $\kappa$ ). Equivalently, no PPT adversary has a non-negligible advantage over random guessing in Game 1.

We complete the proof by reduction. If a PPT forger  $\phi$  with a non-negligible advantage over a random forger exists, one can construct a PPT distinguisher which has a non-negligible advantage over random guessing in Game 1. The exact construction of this distinguisher is given in the full proof of Theorem 1. This contradicts the PRF assumption and hence, no such  $\phi$  exists.  $\square$

### 3.5.5 Failure Scenario

Given a contested object  $I$  generated by author  $i$  and corresponding generation parameters  $\kappa = \langle m, e, r \rangle$ , a failure scenario arises if a random forger is able to sample a  $s \sim \mathcal{D}_0$  such that  $\text{Sim}(I, L_m(e, s))$  is large, with non-negligible probability. In other words, even with a randomly chosen starting point, the random forger is able to generate an object which is highly similar to  $I$  with a non-negligible success rate. In this failure scenario, Assumption A2 is violated and the distribution of  $\text{Sim}(I, L_m(e, s))$  is no longer sub-exponential. In particular, the tail probability  $\mathbb{P}_{s \leftarrow \mathcal{D}_0}[\text{Sim}(I, L_m(e, s)) \geq k]$  does not decay exponentially in  $k$ , as there is a non-negligible measure of starting points  $s \sim \mathcal{D}_0$ , for which  $L_m(e, s)$  outputs an object which is highly similar to  $I$ . Such failure scenario may arise, for example, if the LDM is backdoored [54] or has been trained on insufficient data, leading to memorization [13].

Nonetheless, even in this failure scenario, no PPT adversary has a non-negligible advantage over a random forger. The adversary is still restricted to sampling starting points from the distribution  $G(f_j(\tilde{\kappa}))$ , where  $j$  and  $\tilde{\kappa}$  denote the forger’s identity and forged generation parameters, respectively. By the PRF Assumption A1,  $f_j(\tilde{\kappa})$  is computationally indistinguishable from a uniformly random sequence. Consequently, the adversary is reduced to random sampling from  $\mathcal{D}_0$ , and thus, has a negligible advantage over a random forger.

Moreover, if the PA has access to the same computational resources as the forger, its sampling procedure (Step 2) would likewise encounter starting points corresponding to this failure scenario. As a result, the PA would be able to detect a violation of Assumption A2. As described in Section 3.4, to ensure that the authorship of an object can be attested with

high statistical confidence, the author may also perform independent verification to detect such failure scenarios.

## 4 Analysis of Similarity Function

### 4.1 Similarity of Generated Objects

**Role of the seed** In our POA framework, the seed is constructed by passing the author’s unique identifier and generation parameters into a PRF  $f_i$ . The seed is then passed into a pseudorandom number generator  $G$  to generate an initial random starting point for the diffusion process according to some distribution (e.g. multivariate Gaussian distribution). We can show that two distinct seeds used to generate a random starting point from a standard multivariate Gaussian distribution, then with high probability, normalized squared  $\ell_2$  distance<sup>1</sup> between the two starting points is in the range  $2 \pm 3 \times \sqrt{\frac{8}{d}}$ , where  $d$  is the number of dimensions of the starting point (in Stable Diffusion,  $d = 4 \times 64 \times 64$ ).

### Relationship Between Initial Starting Point and Generated Content

In a typical LDM setup, the initial starting point  $s$  follows a multivariate Gaussian distribution  $\mathcal{N}(0, I)$ . Henceforth, let  $\mathcal{D}_0$  be  $\mathcal{N}(0, I)$ . In this process, small amounts of noise is subtracted from the current state over  $t$  timesteps, resulting in a latent-space representation  $\mathcal{L}_t$  (where  $\mathcal{L}_0 = s$ ). In particular, given a pair of independently generated starting points  $(s, s')$  and their corresponding generated objects  $(\mathcal{L}_t, \mathcal{L}'_t)$ , we have the following.

1. Lemma 1: On expectation, the  $\|\mathcal{L}_t - \mathcal{L}'_t\|_2$  is lower bounded by a constant factor of  $\|s - s'\|_2$ . That is, if  $s$  and  $s'$  are far apart, then  $\mathcal{L}_t$  and  $\mathcal{L}'_t$  will also be far apart.
2. Lemma 2: Under typical LDM architecture, the similarity function between  $\mathcal{L}_t$  and  $\mathcal{L}'_t$ , given by  $\text{Sim}(\mathcal{L}_t, \mathcal{L}'_t) := T = \frac{1}{d} \mathcal{L}_t^T \mathcal{L}'_t$  is closely approximated by a sub-exponential distribution parameterized by the mean and variance parameters described in Assumption A2.
3. Theorem 2: Theorem 2 shows that the test statistic  $\text{Sim}(\mathcal{L}_t, \mathcal{L}'_t)$  can be used as an optimal statistical test for determining whether a given object was generated by a particular author under a given identity and generation parameters.

The full proofs are deferred to the appendix; however, we present the precise theorem and lemma statements here to clarify their role in the theoretical justification of our POA framework.

<sup>1</sup>Normalized squared  $\ell_2$  distance between two vectors of equal lengths  $X$  and  $Y$  is  $\frac{1}{|X|} \sum_{\gamma \in X-Y} \gamma^2$

Under Assumption A1, a forger can do no better than choosing a seed uniformly at random, which corresponds to sampling starting points independently from  $\mathcal{D}_0$ . Hence, Lemma 1 shows that objects generated using randomly selected seeds are expected to be far apart in the  $\ell_2$  metric.

**Lemma 1.** *Let  $s, s'$  denote two initial starting points sampled independently from  $\mathcal{N}(0, I)$ , and  $\mathcal{L}_t, \mathcal{L}'_t$  denote the resulting latents after performing DDIM denoising on  $s, s'$  over  $t$  timesteps. The following relationship holds:*

$$\mathbb{E}[\|\mathcal{L}_t - \mathcal{L}'_t\|_2] \geq f(\alpha_t) \mathbb{E}[\|s - s'\|_2],$$

where  $f(\alpha_t) = \frac{1 - \sqrt{1 - \alpha_t}}{\sqrt{\alpha_t}}$  and  $\alpha_t > 0$  is a small constant from the DDIM scheduler which is decreasing in  $t$ .

Lemma 2 justifies Assumption A2 that the test statistic  $\text{Sim}(\mathcal{L}_t, \mathcal{L}'_t) := T = \frac{1}{d} \mathcal{L}_t^\top \mathcal{L}'_t$  converges to a sub-exponential distribution. When the generated objects  $\mathcal{L}_t$  and  $\mathcal{L}'_t$  correspond to two independently sampled starting points from  $\mathcal{D}_0$ ,  $T$  is a sub-exponential variable with zero mean. In contrast, when  $\mathcal{L}_t$  and  $\mathcal{L}'_t$  are generated from the same starting point,  $T$  has a non-zero mean. This allows us to distinguish between objects generated from the same vs separate randomly chosen starting points.

**Lemma 2.** *Let  $X, Y_1, \dots, Y_n \in \mathbb{R}^d$  be latent vectors produced by the VAE component of an LDM. If  $Y_1, \dots, Y_n$  are generated from different starting points sampled independently from  $\mathcal{D}_0$ , then the inner products  $\{X \cdot Y_i\}_{i=1}^n$  are sub-exponential random variables with mean 0. Otherwise, if  $Y_i$  and  $X$  are generated using the same starting point, prompt, and meta-parameters,  $X \cdot Y_i$  remains sub-exponential but has strictly positive mean.*

In Lemma 2, although  $X \cdot Y_i$  is sub-exponential, its exact distribution does not admit a closed-form expression. For empirical estimation, we approximate its distribution using a generalized normal distribution, which preserves sub-exponential tail behavior and admits a tractable parametric form (see, e.g., [2, 35, 55]). A generalized normal distribution is parameterized by a location parameter (mean)  $\mu$ , scale parameter  $\gamma$  and shape parameter  $\beta$ , which admit maximum likelihood (MLE) estimators. Under standard regularity conditions, the estimation error is bounded by  $O(1/\sqrt{n})$ .

Finally, Theorem 2 presents a statistically optimal test<sup>2</sup> for determining whether a contested object corresponds to a given author and associated generation parameters under a pre-determined false-positive rate. This is achieved by leveraging Lemma 2, and testing whether the similarity score between the contested object and the latent generated by the author’s generation parameters has a statistically significant positive mean.

<sup>2</sup>Statistically optimal in the sense that it is a uniformly most powerful test. Among all tests with a fixed false-positive rate, it achieves the lowest possible false-negative rate.

**Theorem 2.** *Let  $T = \text{Sim}(\mathcal{L}, \mathcal{L}') = \frac{1}{d} \mathcal{L} \cdot \mathcal{L}'$  denote the similarity score between  $\mathcal{L}, \mathcal{L}'$ . Assume that  $\text{Sim}(\mathcal{L}, \mathcal{L}')$  follows a generalized normal distribution with mean  $\mu$ , and common scale and shape parameters  $\gamma$  and  $\beta$ . Consider the hypothesis test  $H_0 : \mu = 0$  ( $\mathcal{L}$  and  $\mathcal{L}'$  are not similar) v.s.  $H_1 : \mu > 0$  ( $\mathcal{L}$  and  $\mathcal{L}'$  are similar), and the test statistic  $T(\mathcal{L}, \mathcal{L}') = 1(\max(0, \text{Sim}(\mathcal{L}, \mathcal{L}')) \geq W_a)$ , where  $W_a$  is the  $(1 - a)$  quantile of  $W$  (as defined in Section 3.4), given  $I$ . It follows that  $T$  is a uniformly most powerful test among all tests with a false-positive rate of at most  $a$ .*

## 4.2 Adversarial Attack on Similarity Function

Given a contested object  $I$ , generated from latent  $\mathcal{L}$ , and its corresponding generation parameters  $\kappa = \langle m, e, r \rangle$ , consider a distance function  $D(\cdot, \cdot)$  over the metric space of  $\mathcal{L}$ , such as the  $\ell_2$  distance. An adversary may attempt an adversarial attack on  $\text{Sim}(\mathcal{L}, \cdot)$ , by finding a  $\tilde{\mathcal{L}}$  s.t.  $D(\mathcal{L}, \tilde{\mathcal{L}})$  is small, but  $\text{Sim}(\mathcal{L}, \tilde{\mathcal{L}})$  is significantly reduced. This causes the judge to fail to attribute  $\tilde{\mathcal{L}}$  to  $\kappa$ .

### 4.2.1 Robustness against Adversarial Attack in $\ell_p$

Suppose the adversary wants to construct a  $\tilde{\mathcal{L}} = \mathcal{L} + v$ , where  $\|v\|_p \leq \epsilon$ , such that the PA computes a low similarity score and high  $\hat{q}_i$ , indicating that  $\tilde{\mathcal{L}}$  is not generated by author  $i$  using generation parameters  $\kappa$ . For any  $p \geq 1$  and  $\|v\|_p \leq \epsilon$ , we show in Appendix D that  $\text{Sim}(\mathcal{L}, \tilde{\mathcal{L}}) \geq \text{Sim}(\mathcal{L}, \mathcal{L}) - \frac{1}{d} \epsilon \|\mathcal{L}\|_q$ , where  $q = \frac{p}{p-1}$ . For example, when  $p = 2, q = 2$  whereas when  $p = 1, q = \infty$ . Furthermore, for all  $q > 1$  (i.e.,  $p < \infty$ ),  $\|\mathcal{L}\|_q \in o(d)$ . Therefore, the impact of  $v$  on the similarity score, for reasonable choices of  $\epsilon$  which preserve perceptual similarity between the generated objects, is negligible.

Since we impose no structural assumptions on the perturbation  $v$  beyond the norm constraint  $\|v\|_p \leq \epsilon$ , the above bound characterizes the worst-case degradation of the similarity score under  $\ell_p$ -bounded adversarial perturbations. We therefore conclude that the similarity function is robust against  $\ell_p$  adversarial perturbations that aim to reduce it (including gradient-based optimizations such as FGSM or PGD).

### 4.2.2 On Geometric Transformations

To evade detection, the forger may attempt a perceptual preserving geometric transformation on the generated object. Unlike  $\ell_p$ -bounded perturbations, geometric distortions induce non-local but structured changes. In this case, a transformation of the forged object  $\mathcal{L}$  may correspond to a transformed version of the original  $L_m(e, f; \kappa)$ . For example, the forged object could be a rotated or scaled version of the original. To mitigate this, the author provides a transformation  $t$  as described in Section 3.4, to align the generated and forged objects prior to comparing similarity. These transformations

are also evaluated by the judge to determine if they are reasonable. Designing similarity functions robust to such distortions remains an open area of research.

## 5 Evaluations

We empirically verify the following:

1. Section 5.2: Distribution of  $\text{Sim}(L_m(e, s_1), L_m(e, s_2))$ , where  $s_1, s_2 \sim \mathcal{D}_0$ , follows a sub-exponential distribution as described in Assumption A2, and can be accurately approximated using small number of samples
2. Section 5.3: The probabilistic adjudicator (PA) described in Section 3.4 is able to accurately verify assertions with high statistical confidence, determining whether a contested object corresponds to a particular author and POA.
3. Section 5.4: The PA is empirically shown to be robust to noise (e.g., additive Gaussian noise and JPEG compression) and perceptually preserving transformations (e.g. cropping, rotation, scaling, translation).

Additionally, Section D.1, empirically verifies  $\ell_2$  distance between generated latents is preserved up to a constant factor relative to their starting points. Appendix E presents representative images generated using our POA scheme.

### 5.1 Experimental Setup

**LDM and datasets** We employed Stable Diffusion 2.1 [39] with its default parameters and VAE as the LDM, which is available from HuggingFace. Images were generated using prompts sourced from the Stable Diffusion Prompt dataset<sup>3</sup>. Finally, we employed the HMAC with SHA-256 hash as our PRF to construct the seed using the the author’s identifier and generation parameters, which is then passed into PyTorch’s Gaussian random generator to sample from  $\mathcal{N}(0, 1)$

**System Configuration** Processor: Intel(R) Xeon(R) CPU E5-2620 v4 @ 2.10GHz; RAM: 256GB; OS: Ubuntu 20.04.4 LTS; GPU: NVIDIA Tesla V100.

**Registration, Generation and Contention** The registration, generation and contention process is described in Section 3.1.2. The specifics of our implementation is described below.

**Registration** An author is assigned a unique randomly sampled integer identifier  $i$ .

<sup>3</sup><https://huggingface.co/datasets/Gustavosta/Stable-Diffusion-Prompts>

**Generation** The author experiments on various LDM parameters  $m$ , prompt embedding  $e$ , and a sequence of random bits  $r$ . Next, compute the seed  $s_{\langle m, e, r \rangle} = f_i(\langle m, e, r \rangle)$ , where  $f_i$  is the HMAC-SHA256 pseudorandom function using  $i$  as the key. Finally, the author generates the starting point  $G(s_{\langle m, e, r \rangle})$ , and uses it to generate the latent space representation  $\mathcal{L}$ , which is then upscaled into the final generated image  $I$  through the VAE. In our evaluations, we employed PyTorch’s Gaussian random number generator as  $G$ , and the default VAE included in the Stable Diffusion 2.1 pipeline.

**Contention** Suppose the author wishes to assert their authorship of an image  $I'$  using the generation parameters  $\kappa = \langle m, e, r \rangle$ . The following is performed:

1. Generate the latent space representation  $\mathcal{L}'$  by passing  $I'$  into the LDM’s VAE encoder.
2. Generate  $\mathcal{L} = L_m(e, G(f_i(\kappa)))$ .
3. Compute the test statistic in Theorem 2 over  $\mathcal{L}$  and  $\mathcal{L}'$ , which is  $T = \frac{1}{d} \mathcal{L}^T \mathcal{L}'$ .

### 5.2 Distribution of Similarity Function

Assumption A2 posits that given a generated object  $I = L_m(e, s_0)$ , the distribution of  $\text{Sim}(I, L_m(e, s))$ , where  $s \sim \mathcal{D}_0$ , follows a sub-exponential distribution. Since the sub-exponential distribution is intractable, we assumed in Section 4.1 that a generalized normal distribution closely approximates this sub-exponential distribution. To validate these two assumptions, we perform the following: Given a fixed prompt embedding  $e$  and model meta-parameters  $m$ ,

1. Independently sample  $s_0, s_1, \dots, s_n \sim \mathcal{N}(0, 1)$ , where  $n = \ln^2 \frac{1}{\alpha} \ln \frac{1}{\delta}$ ,  $\alpha = 2^{-10}$  and  $\delta = 10^{-3}$
2. Generate  $I_0, \dots, I_n$ , where  $I_j = L_m(e, s_j)$  denotes the (flattened) latent generated conditional on  $m, e$  and starting point  $s_j$ .
3. Compute the similarity scores  $T = \text{Sim}(I_0, I_j) = \frac{1}{d} I_0 \cdot I_j$  for  $j = 1, \dots, n$ , where  $d = 4 \times 64 \times 64$ .
4. Approximate the scale, location and shape parameters of the generalized normal distribution.
5. Compute the Kolmogorov-Smirnov (KS) distance between the computed similarity scores and the approximated distribution

This procedure is repeated over 100 text embeddings generated from randomly sampled prompts.

Given two cumulative distribution functions (CDF)  $F$  and  $\hat{F}$  over support  $\mathbb{X}$ , the KS distance between  $F$  and  $\hat{F}$  is:  $KS(F, \hat{F}) = \sup_{x \in \mathbb{X}} |F(x) - \hat{F}(x)|$ . Intuitively,  $KS(F, \hat{F})$  captures the maximum discrepancy between  $F$  and  $\hat{F}$ , small values indicate that the two distributions are close. The mean

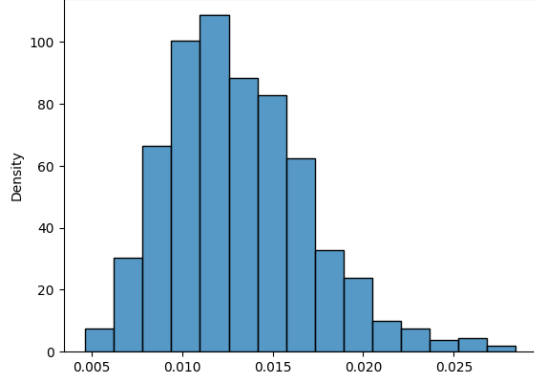


Figure 4: Empirical distribution of KS distances, which observes that the fitted sub-exponential distribution closely approximates the distribution of the similarity scores.

and standard deviation of the KS distances across the 100 embeddings are 0.012 and 0.003, respectively, and the distribution is illustrated in Figure 4. This empirically confirms that the sub-exponential distribution closely approximates the distribution of the similarity scores.

### 5.3 Similarity Function Evaluation

We evaluate similarity metric proposed in Section 4.1 (i.e.  $Sim(X, Y) = \frac{1}{d}X \cdot Y$ ) and the Probabilistic Adjudicator described in Section 3.4 under the following settings:

1. **Clean setting:**  $X$  and  $Y$  are clean and unmodified images generated directly by the LDM
2. **Noise and compression setting:**  $Y$  is obtained from  $X$  by applying Gaussian noise or JPEG compression.
3. **Affine transformation setting:**  $Y$  is obtained from  $X$  via a mild, perceptually preserving affine transformation.

**Clean Performance and Robustness to Noise and Compression** To evaluate the performance of our similarity metric and PA, we proceed as follows. For a  $\delta = 10^{-4}$ , contested object  $I$ , and  $\kappa = \langle m, e, r \rangle$ , we run the PA described in Section 3.4 as follows:

1. Independently sample  $s_1, \dots, s_n \sim \mathcal{N}(0, I)$ , where  $n = \ln^2 \frac{1}{\alpha} \ln \frac{1}{\delta}$ . Compute  $s_0 = G(f_i(\langle m, e, r \rangle))$  as the starting point derived from the authors’s identity and generation parameters.
2. Generate latents  $J_0, \dots, J_n$ , where  $J_j = L_m(e, s_j)$  denotes the flattened latent generated conditional on  $(m, e)$  and starting point  $s_j$ .
3. Compute similarity scores  $Sim(J_0, J_j) = \frac{1}{d}J_0 \cdot J_j$ , for  $j = 1, \dots, n$ , as defined in Section 4.1, where  $d = 4 \times 64 \times 64$ .

4. Fit a generalized normal distribution to the empirical similarity scores using the gennorm function from Python’s scipy library, and estimate the empirical similarity distribution  $\widehat{W}$
5. Compute  $T = Sim(J_0, I)$ . Output  $\hat{q} = \mathbb{P}[\widehat{W} \geq T]$  and its corresponding  $(1 - \delta)$  confidence interval  $C_\delta$

**Judge** Let  $q'$  denote the upper quantile of  $C_\delta$ . We simulate the judge’s decision by accepting the assertion that the contested  $I$  originates from the original  $J_0$ , if  $q' \leq p_r$ , where  $p_r \in \{2^{-10}, 2^{-30}, 2^{-50}\}$ , with a corresponding choice of  $\alpha = p_r/2$ . Recall from Section 3.4 that  $p_r$  upper bounds the probability that a random forger generates an object whose similarity score exceeds the threshold  $T$ , and  $\alpha$  is an upper bound of the estimation error of  $\hat{q}$  with probability at least  $(1 - \delta)$

This procedure is repeated over 100 text embeddings generated from randomly sampled prompts. We consider the following types of distortions applied to  $I_0$ :

- **Gaussian noise:** Add noise sampled from  $\mathcal{N}(0, \sigma^2)$  to the base image, with  $\sigma^2 \in \{1, 3, 9\}$ .
- **JPEG compression:** The decoded image corresponding to  $I_0$  is compressed using JPEG with quality ( $q$ ) parameters 75, 50 and 10, where lower  $q$  indicates higher compression.

### 5.4 Robustness against Affine Transformations

To evaluate robustness against mild geometric distortions, we additionally consider a class of perceptually preserving affine transformations. Specifically, for each original  $I_0$ , we apply a randomly sampled affine transformation parameterized as follows:

- **Scaling (zoom):** A multiplicative scaling factor sampled uniformly from  $[0.98, 1.02]$ , corresponding to a mild zoom of up to  $\pm 2\%$ .
- **Translation:** Horizontal and vertical translations sampled uniformly from  $[-2\%, 2\%]$  of the image dimensions.
- **Rotation:** A rotation angle sampled uniformly from  $[-3^\circ, 3^\circ]$ .
- **Shearing:** A shear angle sampled uniformly from  $[-2^\circ, 2^\circ]$ .

In our evaluations, we assume that the PA can accurately determine the affine transformation used. Let  $t$  be the transformation that aligns the contested  $I$  and the original object  $J_0$  (generated using the author’s identifier and generation parameters). We modify the testing procedure described in Section 5.3, to account for affine perturbations as follows:

- Replace Step (3) with: Compute  $Sim(J_0, t(J_j))$  for  $j = 1, \dots, n$ .
- Replace Step (5) with: Compute  $T = Sim(J_0, t(I))$ . Output  $\hat{q} = \mathbb{P}[\hat{W} \geq T]$  and its corresponding  $(1 - \delta)$  confidence interval  $C_\delta$

The empirical results of the PA under various transformation settings and random forger success probabilities are given in Table 3. Note that the false-reject rate refers to the probability that an object with a valid generation parameters is incorrectly rejected by the judge at a given random forger success rate. Furthermore, during our evaluations, we did not encounter any false positives (i.e. random images which were above the similarity threshold) across all settings. The similarity-score distributions remain well separated and the empirical false-positive rates remain negligible even under substantial noise, compression, and affine perturbations.

Distortion	Distortion Details	Random Forger’s Success Rate $p_r$		
		$2^{-10}$	$2^{-30}$	$2^{-50}$
None	-	0.00	0.00	0.00
Additive Gaussian Noise $\mathcal{N}(0, \sigma^2)$	$\sigma^2 = 1$	0.00	0.00	0.00
	$\sigma^2 = 3$	0.00	0.00	0.00
	$\sigma^2 = 9$	0.00	0.00	0.00
JPEG Compression Quality $q$	$q = 75$	0.00	0.00	0.00
	$q = 50$	0.00	0.00	0.00
	$q = 10$	0.00	0.00	0.01
Random Affine Transformation	-	0.00	0.00	0.00

Table 3: Empirical evaluations of the PA’s similarity-score distributions under clean and distorted inputs. For each distortion, we report the judge false reject rate at random forger success rates  $\{2^{-10}, 2^{-30}, 2^{-50}\}$ . All values are rounded to 2 decimal places.

## 6 Related Work

### 6.1 Digital Watermarking for Authorship Protection

Image watermarking has been a topic of extensive research for several decades, with work as early as 1994 [48]. Early watermarking schemes focus on the post-watermarking setting, where watermarks are embedded in the pixel or frequency domain (e.g. [20, 24]). The latter has been shown to be more robust against mild affine and geometric perturbations. Such watermarking schemes have been used to embed authorship information into digital media, see for example [33, 44].

Recently, there has been growing interest in watermarking AI-generated content, such as the output of large language

models (LLMs) and diffusion models. [23] introduced the notion of undetectable watermarks in LLMs, which embeds the watermark by controlling the model’s pseudorandom number generator. Since then, there has been continued interest in watermarking AIGC, for use cases such as copyright protection and misuse tracking.

Watermarking techniques for AIGC created using LDMs can be broadly categorized as follows.

1. **Post-processing watermarking:** Embeds watermarks directly into generated images using traditional pixel and frequency domain, but is vulnerable to common attacks like removal or ambiguity attacks (see for example [45]).
2. **Fine-tuning-based watermarking:** Modifies the diffusion model to introduce watermarks during generation, and a separate trained detector to extract such watermarks [11, 28]. However, it is possible to remove such watermarks from a model by further fine-tuning them on clean data [18, 19].
3. **Latent space watermarking:** Embeds watermarks in the latent space starting point [14, 50, 53]. Care must be taken when designing such watermarks, as methods like Tree-Ring Watermarking [50], alter the latent distribution, making them detectable via steganographic attacks [51]. Empirical evaluations [14, 42] also show that Gaussian Shading introduces artifacts in the generated images [53] and restricts the diversity of output images [14]. The PRC watermarking scheme [14] is as of now, the only provably undetectable latent space watermarking method, but is only able to encode a limited number ( $\sim 500$ ) of bits robustly if a small amount of white-noise noise is added to the image.

### 6.2 Attacks on Watermarking

Recently, there has been increasing interest in attacks targeting the removal of watermarks from AI Generated Content [32]. Such attacks aim to remove watermarks from a watermarked content while preserving their quality and usability [38]. For instance, [56] demonstrated that traditional post-processing watermarking schemes are vulnerable to re-generation attacks, where a generative AI model is used to create a perceptually similar but unwatermarked version of the image. Post-processing watermarks are also susceptible to ambiguity attacks [7, 29].

Recent research has explored embedding watermarks into the generation process of AIGC by sampling the starting point from a secret watermarked distribution [14, 50, 53]. However, some of these schemes produce outputs which are easily distinguishable with non-watermarked objects [14, 42] and can be removed [26]. Moreover, empirical evaluations of these schemes show that these watermarks can be removed by adding mild white-noise if the message length is too long

(> 1,000 bits) [26]. This limits their effectiveness in encoding authorship information in the generated content.

### 6.3 Authentication of Digital Content

Traditionally, digital content (e.g., a document, video, or digital image) is authenticated by digitally signing the content, which is made public to enable verification. To prove authorship, the digital signature should be timestamped using some verifiable timestamping service (see for example [1, 3]) – which allows the first entity who registered the timestamped signature to be designated as the author.

In settings where the digital content may be altered slightly (e.g. mild noise or compression), this becomes more challenging as small change in the content renders the original signature invalid [17]. Efforts to address this include making such signatures robust against mild compression [10], considering robust (perceptual) hashes which tolerate mild distortions [8, 34], and constructing hashes robust to certain classes of transformations [36]. Nonetheless, some of these approaches suffer from high false reject rates (where two similar content is hashed as not similar) [16] or may be circumvented using perceptual-preserving transformations not considered in the hash – see [31] for an example of such transformation. To date, besides watermarking, we are not aware of existing work which deals with authentication specifically for AI generated content.

## 7 Discussion

### 7.1 Watermarking vs Proof-of-Authorship

A natural question arises: can we leverage existing watermarking techniques to embed POA information into images generated by LDMs, which can be extracted to assert ownership during contention (see, for example, [33, 37])?

Firstly, existing watermarking schemes typically rely on a secret key for watermark generation and decoding. For example, PRC [14], NoisePrints [12] and Gaussian Shading [53] relies on secret keys to ensure undetectability. In contrast, our POA scheme does not rely on any secret. Instead, all POA-related information can be released publicly, enabling transparent and public authorship verification.

As discussed in Section 6.1, existing watermarking approaches are vulnerable to removal and ambiguity attacks, and watermarked models can be effectively de-watermarked. Consequently, watermarking alone may be insufficient to establish authorship with high confidence.

Notably, NoisePrints [12] adopts a parallel approach but is fundamentally different from our framework. In NoisePrints, the initial random starting point is generated by passing a cryptographic hash of a secret as a seed into the starting point sampler. To authenticate a contested object, the object is regenerated using this seed together with the generation parameters,

and the similarity between the contested and regenerated objects is evaluated. In contrast, our POA framework does not rely on any secret. NoisePrints proposes hiding this secret via zero-knowledge proof mechanism – this incurs significant computational overhead [40]. In contrast, our POA framework enables public verification without any cryptographic proof system.

In contrast, our POA framework cryptographically binds an author and generation parameters to an object. Even if an adversary could accurately invert an image to its original latent starting point and knows the seed used, it remains computationally inefficient (due to Assumption A1) to derive another set of generation parameters which maps to the same object under the forger’s identity. Furthermore, our POA framework does not require watermarking the model itself, authorship verification remains possible as long as the original model used is available. Finally, under Assumption A1 (the PRF assumption), the distribution of starting points generated by our framework is computationally indistinguishable from that of truly random starting points. Consequently, objects generated using the POA framework are indistinguishable from those produced by the standard LDM generation process, and therefore do not introduce the visible or statistical artifacts observed in some watermarking schemes.

### 7.2 Practical Considerations

Similar to digital signature-based authentication systems, our framework requires the registration of POA-related information—e.g. the author’s unique ID. This registration can be performed in a timestamped manner, for instance, by recording it in a trusted ledger or through public, verifiable publication.

Secondly, most widely-used LDMs (e.g., various versions of Stable Diffusion) sample the initial latent point from  $\mathcal{N}(0, I)$ . As explained in Section 3.3, our POA framework does not impose any security assumptions on the starting point sampler  $G$ . If a model employs a different starting point distribution,  $G$  can be replaced accordingly, while deriving the seed in the same manner.

## 8 Conclusion

In this paper, we have introduced a proof-of-authorship framework for latent diffusion models. This framework cryptographically binds an author and generation parameters to the generated object. Unlike prior watermarking approaches, no secrets are needed. Furthermore, our analysis shows that no polynomial-time forger can outperform random guessing when attempting to forge a valid assertion for a generated object. Finally, empirical evaluations demonstrate that the framework reliably binds authorship information to generated content, while remaining robust against mild-to-moderate perturbations (e.g. noise, compression, affine transformations).

## References

- [1] Aki. Digital signatures: a tutorial survey. *Computer*, 16(2), 1983.
- [2] Mohammad A Aljarrah, Felix Famoye, and Carl Lee. A new generalized normal distribution: Properties and applications. *Communications in Statistics-Theory and Methods*, 48(18), 2019.
- [3] Kellogg S. Booth. Authentication of signatures using public key encryption. *Communications of the ACM*, 24(11), 1981.
- [4] Mackenzie Caldwell. What Is an “Author”?-Copyright Authorship of AI Art Through a Philosophical Lens. *Houston Law Review*, 61(2), 2023.
- [5] Karni Chagal, Tania Christian, and Patrick Schmitz. Generative ai has an intellectual property problem. *Harvard Business Review*, April 2023.
- [6] Ricky TQ Chen, Xuechen Li, Roger B Grosse, and David K Duvenaud. Isolating sources of disentanglement in variational autoencoders. *NeurIPS*, 2018.
- [7] Scott Craver, Nasir D. Memon, Boon-Lock Yeo, and Minerva M. Yeung. Resolving rightful ownerships with invisible watermarking techniques: limitations, attacks, and implications. *IEEE J. Sel. Areas Commun.*, 16(4), 1998.
- [8] Ling Du, Anthony T.S. Ho, and Runmin Cong. Perceptual hashing for image authentication: A survey. *Signal Processing: Image Communication*, 81, 2020.
- [9] Rick Durrett. *Probability: Theory and Examples*. Cambridge university press, 2019.
- [10] Simon Erfurth. Digital signatures for authenticating compressed JPEG images. Cryptology ePrint Archive, Paper 2024/588, 2024.
- [11] Pierre Fernandez, Guillaume Couairon, Hervé Jégou, Matthijs Douze, and Teddy Furon. The stable signature: Rooting watermarks in latent diffusion models. In *ICCV*, 2023.
- [12] Nir Goren, Oren Katzir, Abhinav Nakarmi, Eyal Ronen, Mahmood Sharif, and Or Patashnik. Noiseprints: Distortion-free watermarks for authorship in private diffusion models. *arXiv preprint arXiv:2510.13793*, 2025.
- [13] Xiangming Gu, Chao Du, Tianyu Pang, Chongxuan Li, Min Lin, and Ye Wang. On memorization in diffusion models. *arXiv preprint arXiv:2310.02664*, 2023.
- [14] Sam Gunn, Xuandong Zhao, and Dawn Song. An undetectable watermark for generative image models. *arXiv preprint arXiv:2410.07369*, 2024.
- [15] Jiayi Guo, Xingqian Xu, Yifan Pu, Zanlin Ni, Chaofei Wang, Manushree Vasu, Shiji Song, Gao Huang, and Humphrey Shi. Smooth diffusion: Crafting smooth latent spaces in diffusion models. In *IEEE/CVF CVPR*, 2024.
- [16] Qingying Hao, Licheng Luo, Steve T.K. Jan, and Gang Wang. It’s not what it looks like: Manipulating perceptual hashing based applications. In *ACM CCS*, 2021.
- [17] Mohamed Hefeeda and Kianoosh Mokhtarian. Authentication schemes for multimedia streams: Quantitative analysis and comparison. *ACM Transactions on Multimedia Computing, Communications, and Applications (TOMM)*, 6(1), 2010.
- [18] Yuepeng Hu, Zhengyuan Jiang, Moyang Guo, and Neil Gong. Stable signature is unstable: Removing image watermark from diffusion models. *arXiv preprint arXiv:2405.07145*, 2024.
- [19] Leixu Huang, Zedian Shao, and Teodora Baluta. Watermark robustness and radioactivity may be at odds in federated learning. *arXiv preprint arXiv:2510.17033*, 2025.
- [20] Mohan S. Kankanhalli, K. R. Ramakrishnan, and Rajmohan. Content based watermarking of images. In *ACM MM*, 1998.
- [21] Hyunjik Kim and Andriy Mnih. Disentangling by factorising. In *ICLR*, 2018.
- [22] Diederik P. Kingma and Max Welling. An introduction to variational autoencoders. *Foundations and Trends® in Machine Learning*, 12(4), 2019.
- [23] John Kirchenbauer, Jonas Geiping, Yuxin Wen, Jonathan Katz, Ian Miers, and Tom Goldstein. A watermark for large language models. In *ICML*, 2023.
- [24] Martin Kutter, Frederic D. Jordan, and Frank Bossen. Digital signature of color images using amplitude modulation. In *Storage and Retrieval for Image and Video Databases 1997*, 1997.
- [25] B. Laurent and P. Massart. Adaptive estimation of a quadratic functional by model selection. *The Annals of Statistics*, 28(5), 2000.
- [26] De Zhang Lee, Han Fang, Hanyi Wang, and Ee-Chien Chang. Removal attack and defense on ai-generated content latent-based watermarking. In *ACM CCS*, 2025.
- [27] Hyomin Lee, Minseon Kim, Sangwon Jang, Jongheon Jeong, and Sung Ju Hwang. Enhancing variational autoencoders with smooth robust latent encoding. *arXiv preprint arXiv:2504.17219*, 2025.

- [28] Liangqi Lei, Keke Gai, Jing Yu, and Liehuang Zhu. Diffusetrace: A transparent and flexible watermarking scheme for latent diffusion model. *arXiv preprint arXiv:2405.02696*, 2024.
- [29] Qiming Li and Ee-Chien Chang. On the possibility of non-invertible watermarking schemes. In *Information Hiding*, 2004.
- [30] Yingyu Liang, Zhizhou Sha, Zhenmei Shi, Zhao Song, Mingda Wan, and Yufa Zhou. Unraveling the smoothness properties of diffusion models: A gaussian mixture perspective. In *IEEE/CVF CVPR*, 2025.
- [31] Ching-Yung Lin and Shih-Fu Chang. A robust image authentication method distinguishing jpeg compression from malicious manipulation. *IEEE Transactions on Circuits and Systems for Video Technology*, 11(2), 2001.
- [32] Nils Lukas, Edward Jiang, Xinda Li, and Florian Kerschbaum. Sok: How robust is image classification deep neural network watermarking? In *IEEE SP*, 2022.
- [33] Agnieszka Malanowska, Wojciech Mazurczyk, Tanya Koochpayeh Araghi, David Megías, and Minoru Kuribayashi. Digital watermarking - A meta-survey and techniques for fake news detection. *IEEE Access*, 12, 2024.
- [34] Sean McKeown and William J Buchanan. Hamming distributions of popular perceptual hashing techniques. *Forensic Science International: Digital Investigation*, 44, 2023.
- [35] Saralees Nadarajah. A generalized normal distribution. *Journal of Applied statistics*, 32(7), 2005.
- [36] Assa Naveh and Eran Tromer. Photoproof: Cryptographic image authentication for any set of permissible transformations. In *IEEE SP*, 2016.
- [37] Thomas Page. Digital watermarking as a form of copyright protection. *Computer Law & Security Report*, 14(6), 1998.
- [38] Qi Pang, Shengyuan Hu, Wenting Zheng, and Virginia Smith. No free lunch in llm watermarking: Trade-offs in watermarking design choices. *Advances in Neural Information Processing Systems*, 2024.
- [39] Robin Rombach, Andreas Blattmann, Dominik Lorenz, Patrick Esser, and Björn Ommer. High-resolution image synthesis with latent diffusion models. In *IEEE/CVF CVPR*, 2022.
- [40] Saichand Samudrala, Jiawen Wu, Chen Chen, Haoxuan Shan, Jonathan Ku, Yiran Chen, and Jeyavijayan Rajendran. Performance analysis of zero-knowledge proofs. In *IEEE IISWC*, 2024.
- [41] Jun Shao. *Mathematical Statistics*. Springer New York, 2003.
- [42] Kareem Shehata, Aashish Kolluri, and Prateek Saxena. Clue-mark: Watermarking diffusion models using clw. *arXiv preprint arXiv:2411.11434*, 2024.
- [43] Xinyue Shen, Yiting Qu, Michael Backes, and Yang Zhang. Prompt stealing attacks against {Text-to-Image} generation models. In *USENIX Security*, 2024.
- [44] Nicholas Paul Sheppard, Reihaneh Safavi-Naini, and Philip Ogunbona. Secure multimedia authoring with dishonest collaborators. *EURASIP Journal on Advances in Signal Processing*, 2004(14):657830, 2004.
- [45] Chunlin Song, Sud Sudirman, Madjid Merabti, and David Llewellyn-Jones. Analysis of digital image watermark attacks. In *IEEE CCNC*, 2010.
- [46] Jiaming Song, Chenlin Meng, and Stefano Ermon. Denoising diffusion implicit models. In *ICLR*, 2021.
- [47] Mani Valletti, Maxim Ziatdinov, Yongtao Liu, and Sergei V Kalinin. Physics and chemistry from parsimonious representations: image analysis via invariant variational autoencoders. *npj Computational Materials*, 10(1), 2024.
- [48] R.G. van Schyndel, A.Z. Tirkel, and C.F. Osborne. A digital watermark. In *Proceedings of 1st International Conference on Image Processing*, volume 2, 1994.
- [49] Hao Wang. Authorship of artificial intelligence-generated works and possible system improvement in china. *Beijing Law Review*, 14(2), 2023.
- [50] Yuxin Wen, John Kirchenbauer, Jonas Geiping, and Tom Goldstein. Tree-ring watermarks: Fingerprints for diffusion images that are invisible and robust. *arXiv preprint arXiv:2305.20030*, 2023.
- [51] Pei Yang, Hai Ci, Yiren Song, and Mike Zheng Shou. Can simple averaging defeat modern watermarks? In *NeurIPS*, 2024.
- [52] Zhantao Yang, Ruili Feng, Han Zhang, Yujun Shen, Kai Zhu, Lianghua Huang, Yifei Zhang, Yu Liu, Deli Zhao, Jingren Zhou, et al. Lipschitz singularities in diffusion models. In *ICLR*, 2023.
- [53] Zijin Yang, Kai Zeng, Kejiang Chen, Han Fang, Weiming Zhang, and Nenghai Yu. Gaussian shading: Provable performance-lossless image watermarking for diffusion models. In *IEEE/CVF CVPR*, 2024.
- [54] Shengfang Zhai, Yinpeng Dong, Qingni Shen, Shi Pu, Yuejian Fang, and Hang Su. Text-to-image diffusion models can be easily backdoored through multimodal data poisoning. In *ACM MM*, 2023.

- [55] Yiyang Zhang, Zhigang Jin, and Seyedali Mirjalili. Generalized normal distribution optimization and its applications in parameter extraction of photovoltaic models. *Energy Conversion and Management*, 224, 2020.
- [56] Xuandong Zhao, Kexun Zhang, Zihao Su, Saastha Vasani, Ilya Grishchenko, Christopher Kruegel, Giovanni Vigna, Yu-Xiang Wang, and Lei Li. Invisible image watermarks are provably removable using generative ai. In *NeurIPS*, 2024.

## A Estimating $q$

As described in Section 3.1.3, given a pre-specified false-positive rate  $\alpha$  and confidence  $1 - \delta$ , the PA estimates a  $(1 - \delta)$  confidence interval for  $q$ . Leveraging Assumption A2, together with the mild assumptions that the sub-exponential tail is modeled by a generalized normal distribution (as is common in practice as discussed in Section 4.1) and that standard MLE regularity conditions hold, we show below that  $n \in \Omega\left(\ln^2 \frac{1}{\alpha} \ln \frac{1}{\delta}\right)$  independent samples suffices. This result is formally stated as Theorem 3. Henceforth, we will set the number of Monte-Carlo samples used by the PA (as described in Section 3.4) to estimate the similarity distribution to  $n = \ln^2 \frac{1}{\alpha} \ln \frac{1}{\delta}$ , which ensures that for a given  $\alpha$ , the estimation error of  $q$  is upper bounded by  $\Delta q \leq \frac{q}{5}$  with probability at least  $1 - \delta$

**Theorem 3.** *Let  $x_1, \dots, x_n$  be independent and identically distributed realizations of random variable  $X$ , which follows a Generalized Normal Distribution, parameterized by location, shape and scale parameters  $\theta = (\mu, \gamma, \beta)$ . For a fixed  $\alpha \in (0, 1)$  and  $T \in \text{supp}(X)$ , let  $q(\theta) = \mathbb{P}[X \geq T]$ . To determine if  $q(\theta) \leq \alpha$  and upper bound the estimation error of  $q(\theta)$  as  $\Delta q \leq \alpha$  with probability at least  $1 - \delta$ , it suffices to use*

$$n \in \Omega\left(\ln^2 \frac{1}{\alpha} \ln \frac{1}{\delta}\right)$$

samples.

*Proof.* Let  $\hat{\theta}$  be the MLE approximation of  $\theta$ , and let  $f(x; \theta)$  and  $F(x; \theta)$  denote the probability and cumulative distribution function, conditional on parameters  $\theta$ . Without loss of generality, assume that  $\mu = 0$ .

Consider the relative error due to estimation error of  $\theta$  can be estimated using the Delta method as

$$\Delta q \approx \frac{\partial q}{\partial \theta} \|\theta - \hat{\theta}\|_2, \quad (2)$$

see Corollary 1.1 of [41] for more details. It now remains to

bound  $\frac{\partial q}{\partial \theta}$  and  $\|\theta - \hat{\theta}\|_2$ . To bound  $\frac{\partial q}{\partial \theta}$ , first observe that

$$\begin{aligned} \frac{\partial q}{\partial \theta} &= -\frac{\partial F(T; \theta)}{\partial \theta} \\ &= -\frac{\partial}{\partial \theta} \int_{-\infty}^T f(x; \theta) dx \\ &= -\frac{\partial}{\partial \theta} \left(1 - \int_T^{\infty} f(x; \theta) dx\right) \\ &= \frac{\partial}{\partial \theta} \int_T^{\infty} f(x; \theta) dx. \end{aligned} \quad (3)$$

Furthermore, we have

$$\frac{\partial f(x; \theta)}{\partial \theta} = f(x; \theta) \frac{\partial \ln f(x; \theta)}{\partial \theta}, \quad (4)$$

Substituting (4) into (3), we have

$$\begin{aligned} \frac{\partial q}{\partial \theta} &= \int_T^{\infty} f(x; \theta) \frac{\partial \ln f(x; \theta)}{\partial \theta} dx \\ &= \mathbb{E} \left[ \frac{\partial \ln f(X; \theta)}{\partial \theta} \mathbf{1}(X \geq T) \right] \\ &= q \mathbb{E} \left[ \frac{\partial \ln f(X; \theta)}{\partial \theta} \middle| X \geq T \right] \end{aligned} \quad (5)$$

where expectation is over  $X$  which follows a GND distribution parameterized by  $\theta$ . Since  $\ln f(X; \theta) = C_{\gamma, \beta} - K_{\gamma, \beta} X^\beta$ , where  $C_{\gamma, \beta}$  and  $K_{\gamma, \beta}$  are constants depending on  $\gamma$  and  $\beta$ , it follows that  $\frac{\partial \ln f(X; \theta)}{\partial \theta} \in O(X^\beta)$ . By the tail bound of sub-exponential distributions, we have  $q(\theta) = \mathbb{P}[X \geq T] \leq \exp(-K_{\gamma, \beta} X^\beta)$ , or equivalently,  $\ln \frac{1}{q(\theta)} \geq K_{\gamma, \beta} X^\beta$ . Thus,

$$\frac{\partial \ln f(X; \theta)}{\partial \theta} \in O\left(\ln \frac{1}{q(\theta)}\right). \quad (6)$$

Substituting (6) into (5) yields

$$\frac{\partial q}{\partial \theta} \lesssim q \ln \left(\frac{1}{q}\right). \quad (7)$$

Next, we bound  $\|\theta - \hat{\theta}\|_2$ , where  $\hat{\theta}$  corresponds to the MLE estimate of  $\theta$ . Under standard MLE regularity conditions, we have  $\hat{\theta} \sim \mathcal{N}\left(0, \frac{1}{n} I(\theta)^{-1}\right)$ , where  $n$  denotes the number of independent samples used to estimate  $\hat{\theta}$ , and  $I(\theta)$  is the Fisher information of  $\theta$ . Equivalently, we have  $Z = \sqrt{n}(\hat{\theta} - \theta) \sim \mathcal{N}(0, \Sigma)$ , where  $\Sigma = I(\theta)^{-1}$ .

Consider the eigendecomposition  $\Sigma = U \Lambda U^T$ , and transformation  $Y = \Lambda^{-1/2} U^T Z$ . Since  $\mathbb{E}[Y] = \Lambda^{-1/2} U^T 0 = 0$ , and  $\text{Cov}(Y) = \Lambda^{-1/2} U^T \Sigma (\Lambda^{-1/2} U^T)^T = I$ , we have that  $Y \sim \mathcal{N}(0, I)$ . Since  $\dim(\theta) = 3$ , it follows that  $Y^T Y \sim \chi_3^2$ . Next, we observe that  $Z^T Z = Y^T \Lambda Y \leq \lambda_{\max} Y^T Y$ , where  $\lambda_{\max}$  is the largest eigenvalue of  $I(\theta)^{-1}$ . Therefore, we have  $\|\hat{\theta} - \theta\|_2^2 \leq \frac{\lambda_{\max}}{n} Y^T Y$ . Thus, with probability at least  $1 - \delta$ , it follows that

$$\|\hat{\theta} - \theta\|_2 \leq \sqrt{\frac{\lambda_{\max}}{n} \chi_{3, 1-\delta}^2} \lesssim \sqrt{\frac{\lambda_{\max}}{n} \left(3 + \ln \frac{1}{\delta}\right)} \quad (8)$$

where  $\chi_{3,1-\delta}^2$  denotes the  $1 - \delta$  quantile of the  $\chi_3^2$  distribution, and the rightmost bound is due to the Laurent-Massart bound (see Lemma 1 of [25]).

Substituting (7) and (8) into (2), we obtain

$$\Delta q \lesssim q \ln \left( \frac{1}{q} \right) \sqrt{\frac{\lambda_{\max}}{n} \left( 3 + \ln \frac{1}{\delta} \right)}$$

Finally, by Assumption A2, the similarity scores follow a sub-exponential distribution. This implies finite second moments and, consequently, a bounded second moment of the score function. As a result, the Fisher information matrix has bounded operator norm, and in particular its largest eigenvalue  $\lambda_{\max}$  is finite. Thus, we have,

$$\Delta q \in O \left( q \ln \frac{1}{q} \sqrt{\frac{1}{n} \ln \frac{1}{\delta}} \right).$$

To bound  $\Delta q \leq \alpha$ , it suffices for

$$n = \Omega \left( \ln^2 \frac{1}{\alpha} \ln \frac{1}{\delta} \right)$$

□

## B Proof of Theorem 1

To formalize the impossibility of a polynomial-time forger over a random forger with non-negligible advantage, consider the following variant of the PRF Indistinguishability game:

**Game 1** (PRF Indistinguishability Over Chosen Input). *The challenger and adversary interact as follows:*

1. The challenger fixes  $i, m$  and  $e$ , and uniformly samples  $r$
2. The adversary is given  $(i, m, e, r)$ .
3. The adversary is allowed a polynomial number of queries to  $f_i(\cdot)$  on any inputs of its choice, **except** the challenge input  $\langle m, e, r \rangle$ .
4. Challenger samples  $b_0 \leftarrow \text{Unif}(\{0, 1\}^n)$ , and  $b_1 = f_i(\langle m, e, r \rangle)$ , where  $b_0$  and  $b_1$  are both  $n$ -bit sequences.
5. The challenger samples  $\sigma \leftarrow \text{Unif}(\{0, 1\})$  and sends  $b_\sigma$  to the adversary.
6. Adversary outputs  $\hat{\sigma}$  and wins if and only if  $\hat{\sigma} = \sigma$ .

By the PRF assumption, no polynomial-time adversary has a non-negligible advantage over random guessing in Game 1. In Theorem 1 below, we show that no polynomial-time forger can obtain a non-negligible advantage over a random forger. The proof is by reduction, if such a forger exists, one could construct a polynomial-time adversary that wins Game 1 with non-negligible advantage over random guessing, which contradicts the PRF assumption.

**Theorem** (Theorem 1 restated). *Under the PRF assumption, for all polynomial-time forger  $\phi$ ,  $I, \kappa, \delta$  and  $\alpha$ ,  $\text{Adv}_\phi(I, \kappa, \alpha, \delta) \leq \text{negl}(\lambda)$ , where  $\lambda$  is the security parameter of the PRF family.*

*Proof.* Suppose such a PPT forger  $\phi$  exists, and  $\text{Adv}_\phi(I, \kappa) = \beta$  for some non-negligible  $\beta$  (w.r.t  $\lambda$ ). We will show that given a fixed  $m, e, i$  over varying  $r$ ,  $\phi$  can be used to construct a polynomial-time distinguisher which has a non-negligible advantage over random guessing in Game 1.

Since  $f_j$  is an independently keyed instance of a PRF family, we fix the forger's identity to be  $j$  without loss of generality. Recall that forger outputs  $\tilde{\kappa} = \langle \tilde{m}, \tilde{e}, \tilde{r} \rangle$  which corresponds to the forged object  $L_{\tilde{m}}(\tilde{e}, G(f_j(\tilde{\kappa})))$ .

Let  $\mathcal{B} \leftarrow \text{Unif}(n)$  denote a uniformly sampled  $n$ -bit binary string. By the PRF assumption (Assumption A1),  $\mathcal{B}$  and  $\mathcal{B}_\phi := f_j(\tilde{\kappa})$  are computationally indistinguishable. Since  $G$  and  $L_m$  are deterministic, the distributions of the generated objects  $L_m(e, G(\mathcal{B}))$  and  $L_m(e, G(\mathcal{B}_\phi))$  are computationally indistinguishable. Hence, no PPT algorithm  $\phi$  has a non-negligible advantage over random guessing in deriving a  $\tilde{\kappa}$  such that  $L_m(e, G(\mathcal{B}))$  and  $L_m(e, G(\mathcal{B}_\phi))$  are similar.

Suppose such a  $\phi$  exists, a PPT algorithm which has a non-negligible advantage in Game 1 can be constructed using  $\phi$  as follows – In (5) of Game 1, consider an adversary which interacts with  $\phi$  in the following way:

1.  $\phi$  receives  $\kappa = \langle m, e, r \rangle$  and  $I' = L_m(e, b_\sigma)$
2.  $\phi$  attempts to forge a valid generation  $\tilde{\kappa} = \langle \tilde{m}, \tilde{e}, \tilde{r} \rangle$  for  $I'$

Finally, the adversary outputs  $\hat{\sigma} = 1$  if  $S_{\tilde{m}, \tilde{e}, I'}^{\tilde{m}, \tilde{e}, I'}(\tilde{r}) - S_i^{m, e, I}(r) > 0$ . Else, the adversary outputs  $\hat{\sigma} = 0$ .

If  $b_\sigma = f_i(\langle m, e, r \rangle)$ , by the definition of  $\text{Adv}_\phi(I, \kappa)$ , we have  $\mathbb{P}[\hat{\sigma} = 0 | \sigma = 0] = \frac{1}{2} + \beta$ . Else, if  $b_\sigma$  is a randomly sampled sequence,  $\mathbb{P}[\hat{\sigma} = 1 | \sigma = 1] = \frac{1}{2}$ . Hence,

$$\begin{aligned} \mathbb{P}[\hat{\sigma} = \sigma] &= \mathbb{P}[\hat{\sigma} = 1 | \sigma = 1] \mathbb{P}[\sigma = 1] + \mathbb{P}[\hat{\sigma} = 0 | \sigma = 0] \mathbb{P}[\sigma = 0] \\ &= \frac{1}{2} \left( \frac{1}{2} + \beta \right) + \frac{1}{2} \left( \frac{1}{2} \right) \\ &= \frac{1}{2} (1 + \beta), \end{aligned}$$

and thus,  $\phi$  has a non-negligible  $\frac{\beta}{2}$  advantage over random guessing in Game 1. This contradicts the fact that  $f_i$  is a PRF, and hence, no polynomial-time adversary has a non-negligible advantage over random guessing. Hence, there does not exist a PPT forger  $\phi$  with non-negligible  $\text{Adv}_\phi(I, \kappa)$ . □

The intuition behind Theorem 1 is as follows: Regardless of how a PPT forger (with identity  $j$ ) derives an alternative set of generation parameters  $\kappa' = \langle m', e', r' \rangle$  such that  $L_{m'}(e', G(f_j(\kappa')))$  is similar to the original object, the forger still has to sample the starting point  $G(f_j(\kappa'))$ . By the PRF

assumption, this is computationally indistinguishable from  $G(u)$ , where  $u$  is drawn uniformly at random. Since the forger is effectively forced to sample the starting point at random from  $\mathcal{D}_0$ , the  $\ell_2$  distance between  $G(f_i(\kappa))$  and  $G(f_j(\kappa'))$  is  $\Omega(\sqrt{d})$  with high probability. Therefore, by Lemma 1, the resulting generated objects will not be similar with high probability.

## C Proofs in Section 4.1

**Lemma (Lemma 1 restated).** *Let  $s, s'$  denote two initial starting points sampled independently from  $\mathcal{N}(0, I)$ , and  $\mathcal{L}_t, \mathcal{L}'_t$  denote the resulting latents after performing DDIM denoising on  $s, s'$  over  $t$  timesteps. The following relationship holds:*

$$\mathbb{E}[\|\mathcal{L}_t - \mathcal{L}'_t\|_2] \geq f(\alpha_t) \mathbb{E}[\|s - s'\|_2],$$

where  $f(\alpha_t) = \frac{1 - \sqrt{1 - \alpha_t}}{\sqrt{\alpha_t}}$  and  $\alpha_t > 0$  is a small constant from the DDIM scheduler which is decreasing in  $t$ .

*Proof.* If the DDIM scheduler is used, the relationship between  $\mathcal{L}_t$  and  $s$  is given in [46] (Equation (4)):

$$s = \sqrt{\alpha_t} \mathcal{L}_t + \sqrt{1 - \alpha_t} \varepsilon, \quad (9)$$

where  $\alpha_t \in (0, 1)$  is a scheduler-specific constant decreasing in  $t$ . From (9),

$$s - s' = \sqrt{\alpha_t} (\mathcal{L}_t - \mathcal{L}'_t) + \sqrt{1 - \alpha_t} (\varepsilon - \varepsilon'),$$

where  $\varepsilon' = \frac{s' - \sqrt{\alpha_t} \mathcal{L}'_t}{\sqrt{1 - \alpha_t}}$  (from (9)). From the triangle inequality,

$$\|s - s'\|_2 \leq \sqrt{\alpha_t} \|\mathcal{L}_t - \mathcal{L}'_t\|_2 + \sqrt{1 - \alpha_t} \|\varepsilon - \varepsilon'\|_2. \quad (10)$$

Since both  $s - s'$  and  $\varepsilon - \varepsilon'$  are  $\mathcal{N}(0, 2I)$  random variables,  $\mathbb{E}[\|s - s'\|_2] = \mathbb{E}[\|\varepsilon - \varepsilon'\|_2]$ . Therefore, taking the expectation on (10) and rearranging the terms, the bound follows.  $\square$

**Lemma (Lemma 2 restated).** *Let  $X, Y_1, \dots, Y_n \in \mathbb{R}^d$  be latent vectors produced by the VAE component of an LDM. If  $Y_1, \dots, Y_n$  are generated from different starting points sampled independently from  $\mathcal{D}_0$  (possibly under the same prompt and meta-parameters), then the inner products  $X \cdot Y_{i=1}^n$  are sub-exponential random variables with mean 0. Otherwise, if  $Y_i$  and  $X$  are generated using the same starting point, prompt, and meta-parameters,  $X \cdot Y_i$  remains sub-exponential but has strictly positive mean.*

*Proof.* By the VAE training objective (as described in Section 2.1.1), the unconditional prior distribution of VAE latent space follows a  $\mathcal{N}(0, I)$  distribution. Thus, the inner product  $X \cdot Y_i$  is the sum of  $d$  sub-exponential random variables of expectation 0, which is thus sub-exponential with mean 0. On the other hand, if  $X$  and  $Y_i$  are generated using the same starting point, prompt, and meta-parameters,  $X \cdot Y_i$  is the sum of  $d$  sub-exponential and positively correlated random variables, which therefore admits a positive mean.  $\square$

**Theorem (Theorem 2 restated).** *Let  $\text{Sim}(Z_1, Z_2) = \frac{1}{d} Z_1 \cdot Z_2$  denote the similarity score between the latent vectors  $Z_1$  and  $Z_2$ . For tractability, assume that  $\text{Sim}(Z_1, Z_2)$  follows a generalized normal distribution with mean  $\mu$ , and common scale and shape parameters  $\gamma$  and  $\beta$ . Consider the hypothesis test  $H_0 : \mu = 0$  (dissimilar latents) v.s.  $H_1 : \mu > 0$  (similar latents), and the test statistic  $T(Z_1, Z_2) = 1(\max(0, \text{Sim}(Z_1, Z_2)) \geq W_\alpha^1)$ , where  $W_\alpha^1$  is the  $(1 - \alpha)$  quantile of  $W$  (as defined in Section 3.4), given  $I$ . It follows that  $T$  is a uniformly most powerful test among all tests with a false-positive rate of at most  $\alpha$ .*

*Proof.* Under the assumption that  $q = \max(0, \text{Sim}(Z_1, Z_2))$  follows a generalized normal distribution, and admits pdf  $f(x; \mu, \gamma, \beta) \propto \exp\left(-\left(\frac{|x - \mu|}{\gamma}\right)^\beta\right)$ . Consider the following likelihood ratio computed over one pair  $(Z_1, Z_2)$ ,

$$\begin{aligned} l(q) &= \frac{\sup_{\mu \in H_1 \cup H_0} f(q; \mu, \gamma, \beta)}{\sup_{\mu \in H_0} f(q; \mu, \gamma, \beta)} \\ &= \frac{f(q; q, \gamma, \beta)}{f(q; 0, \gamma, \beta)} \\ &= \exp\left(\left(\frac{q}{\gamma}\right)^\beta\right), \end{aligned}$$

which is monotonically increasing in  $q$ . Thus, by the Neymann-Pearson lemma, the test  $T(Z_1, Z_2) = 1(q > W_\alpha^1)$  is the uniformly most powerful test of power  $\alpha$  for  $H_0$  against  $H_1$ .  $\square$

## D $\ell_p$ Adversarial Perturbations on Similarity Function

We discuss the performance of  $\ell_p$  bounded adversaries, for general  $p \geq 1$ . The notations will be reused from Section 4.2. Recall that for a given  $p$ , the adversary constructs  $\tilde{\mathcal{L}} = \mathcal{L} + v$ , subject to the constraint  $\|v\|_p \leq \varepsilon$ , with the goal of minimizing  $\text{Sim}(\mathcal{L}, \tilde{\mathcal{L}}) = \frac{1}{d} (\mathcal{L} \cdot \mathcal{L} + \mathcal{L} \cdot v)$ .

For a given  $p \geq 1$ , define its Holder conjugate  $q = \frac{p}{p-1}$ . By dual-norm of  $\ell_p$  spaces, it can be shown that  $|\mathcal{L} \cdot v| \leq \varepsilon \|\mathcal{L}\|_q$ .

Denote  $v_i$  as the  $i$ -th coordinate of  $v$ . It can be shown that

$$v_i = -\varepsilon \frac{\text{sign}(\mathcal{L}_i) |\mathcal{L}_i|^{q-1}}{\|\mathcal{L}\|_q^{q-1}},$$

for  $i = 1, \dots, d$  attains the minimum value  $\mathcal{L} \cdot v = -\varepsilon \|\mathcal{L}\|_q$ , and minimizes  $\text{Sim}(\mathcal{L}, \tilde{\mathcal{L}}) = \text{Sim}(\mathcal{L}, \mathcal{L}) - \frac{1}{d} \varepsilon \|\mathcal{L}\|_q$ . Thus, at  $p = 1$ ,  $\text{Sim}(\mathcal{L}, \tilde{\mathcal{L}}) = \text{Sim}(\mathcal{L}, \mathcal{L}) - \frac{1}{d} \varepsilon \|\mathcal{L}\|_1$ . Furthermore, it is also straightforward to show that  $\|\mathcal{L}\|_q \in o(d)$ . Thus for reasonable values of  $\varepsilon$  which preserves similarity between  $\mathcal{L}$  and  $\tilde{\mathcal{L}}$ , the impact of  $\frac{1}{d} \varepsilon \|\mathcal{L}\|_q$  on the overall similarity is negligible.

## D.1 Distance Preservation Between Starting Points and Latents

We empirically validate Lemma 1 by showing that the distance between generated latents  $\mathcal{L}_i$  and  $\mathcal{L}_i'$  admits a constant-factor lower bound in terms of the distance between their respective starting points  $s$  and  $s'$ . More specifically, given a pair of text embedding  $e$  and LDM meta-parameter  $m$ ,

1. Randomly sample 30 starting points  $s_1, \dots, s_{30}$  independently from  $\mathcal{N}(0, I)$
2. Generate the 30 corresponding latents  $\mathcal{L}_1^1, \dots, \mathcal{L}_1^{30}$ , where  $\mathcal{L}_i^i = L_m(e, s_i)$  denotes the latent generated using the LDM conditional on  $e, m$  and starting point  $s_i$ .
3. Compute all  $\binom{30}{2}$  pairwise ratios of  $\ell_2$  distances  $\frac{\|\mathcal{L}_i^i - \mathcal{L}_j^j\|_2}{\|s_i - s_j\|_2}$  for  $1 \leq i < j \leq 30$ .

This procedure is repeated over 30 text embeddings derived from prompts randomly sampled from the prompt dataset. The resulting empirical distribution of the distance ratios has mean 4.27 and standard deviation 0.44, and is illustrated in Figure 5. This empirically validates our claim in Lemma 1 that pairwise distances between generated latents are lower bounded by a constant factor of the distances between their initial starting points.

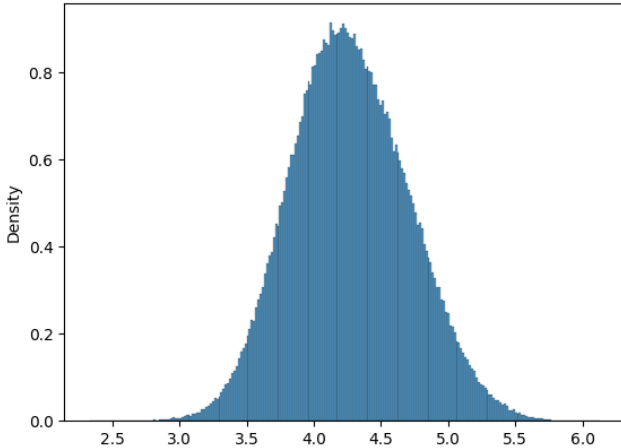


Figure 5: Distribution of the ratio between pairwise  $\ell_2$  distances of generated latents and the corresponding  $\ell_2$  distances between their starting points.

## E Impact of POA Scheme on Generation Process

In our empirical evaluations, we only modified the  $\mathcal{N}(0, I)$  sampling function of the LDM, leaving all other components

unchanged. Therefore, we expect this scheme to work seamlessly for all LDMs which samples a random starting point from this distribution.

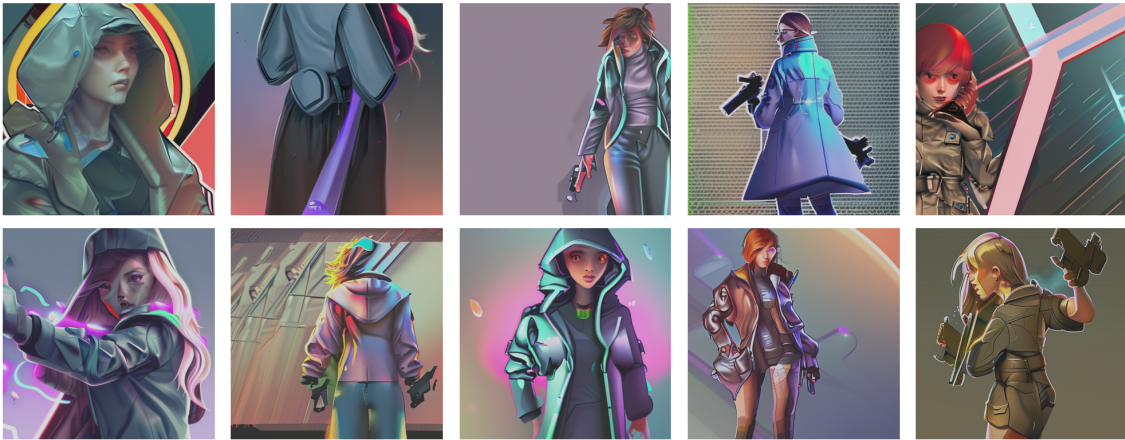
Existing watermarking methods, such as Gaussian shading and tree-ring, have been shown to introduce detectable artifacts and can be easily removed. In contrast, since the  $\mathcal{N}(0, I)$  sampling function relies on a PRG, we do not face these issues.

Recall that in the POA framework, the random starting point is generated by passing  $f_i(\langle m, e, r \rangle)$  into the PRG. Diversity in the generated outputs can still be ensured by varying the free bits  $r$ , even when the prompt and embedding remain fixed. By the PRF assumption, as  $r$  varies, the values  $f_i(\langle m, e, r \rangle)$  are computationally indistinguishable from truly random strings. Consequently, the resulting starting points generated by the POA scheme are indistinguishable from those obtained using truly random seeds.

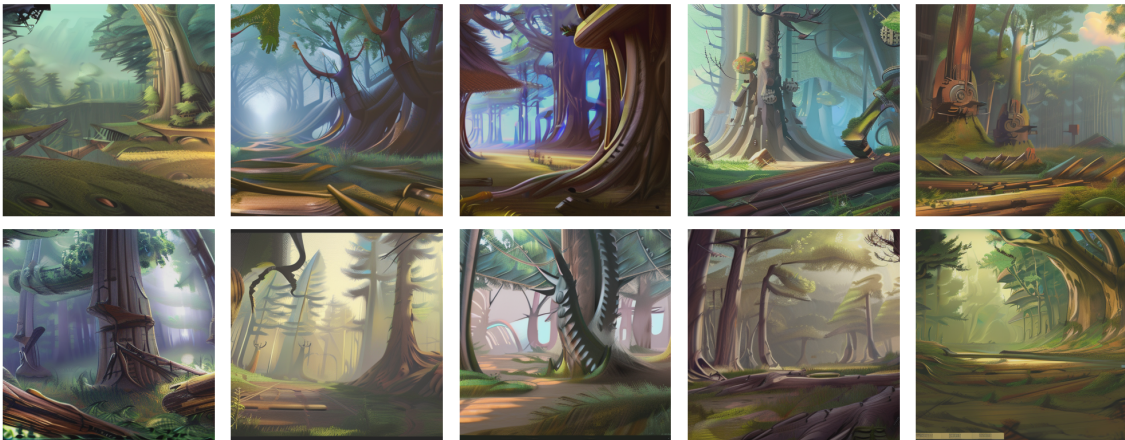
Figure 6 illustrates examples of images generated with identical prompts and meta-parameters but different values of  $r$ .



(a) “steampunk market interior, colorful, 3 d scene, greg rutkowski, zabrocki, karlkka, jayison devadas, trending on artstation, 8 k, ultra wide angle, zenith view, pincushion lens effect”



(b) “girl in a futuristic raincoat, holding a revolver, character concept art, valorant game style, digital art, many details, super realistic, high quality, 8 k”



(c) “good day, morning, landscape, no people, no man, steampunk, forest, wood, lost world, Anime Background, concept art, illustration,smooth, sharp focus, intricate, super wide angle, trending on artstation, trending on deviantart, 4K”

Figure 6: Examples of images generated using the same and meta-parameters  $m$  and prompt embeddings  $e$  (the individual prompts are given in the captions) but different free-bits  $r$ . Despite fixed conditioning, variation in  $r$  yields diverse outputs as each different  $r$  corresponds to a diferent starting point independently sampled from  $\mathcal{N}(0, I)$ .